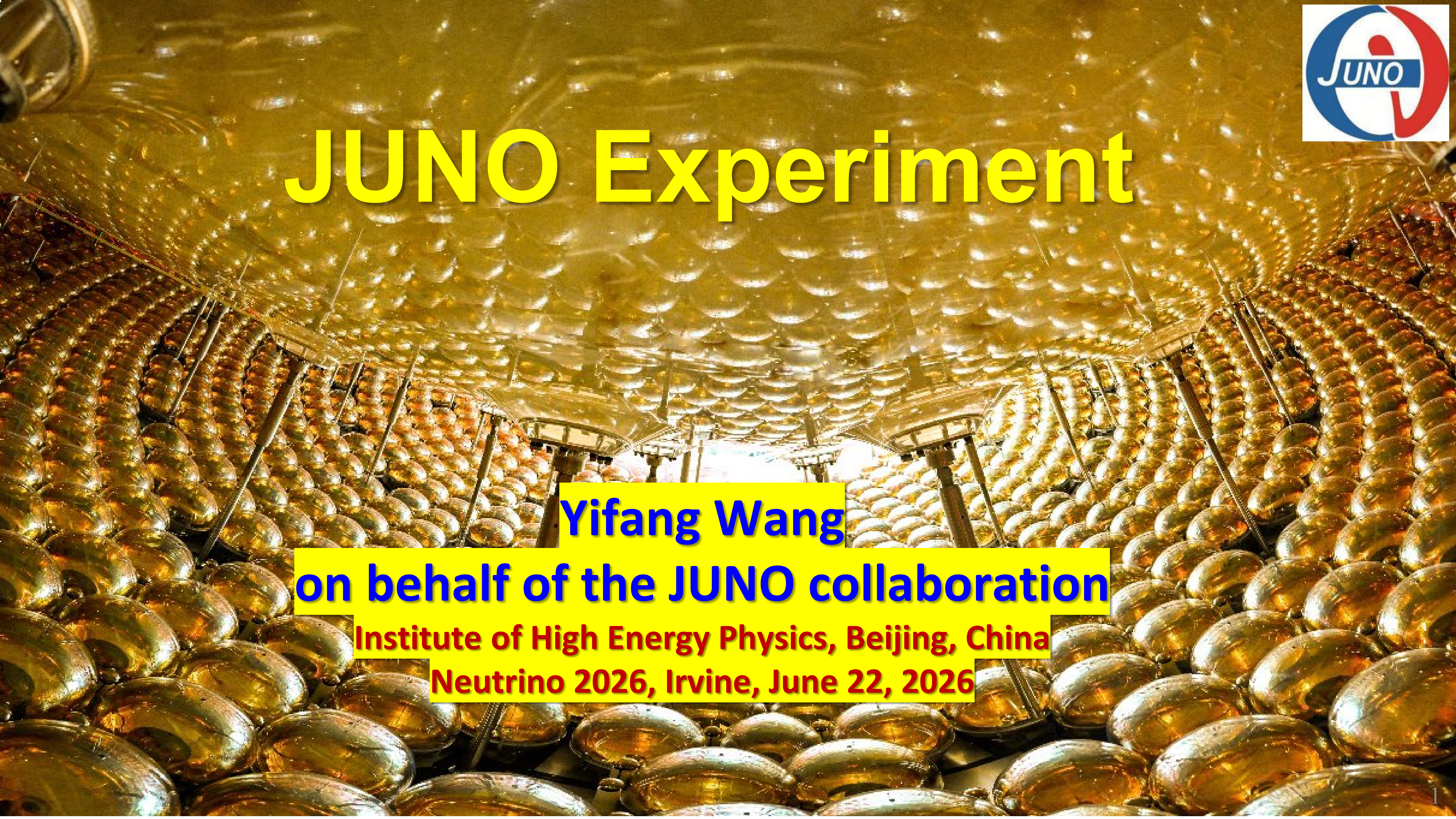

JUNO Experiment

Yifang Wang

on behalf of the JUNO collaboration

Institute of High Energy Physics, Beijing, China

Neutrino 2026, Irvine, June 22, 2026

Content

- Introduction of the JUNO experiment
- Performance of the detector
- New results
- Summary

Idea of the JUNO Experiment

- Use reactor neutrinos to determine the mass ordering (sign of Δm^2_{32}), independent of matter effects and CP phase δ
- Equal distance to two reactor power plants for doubling the ν flux

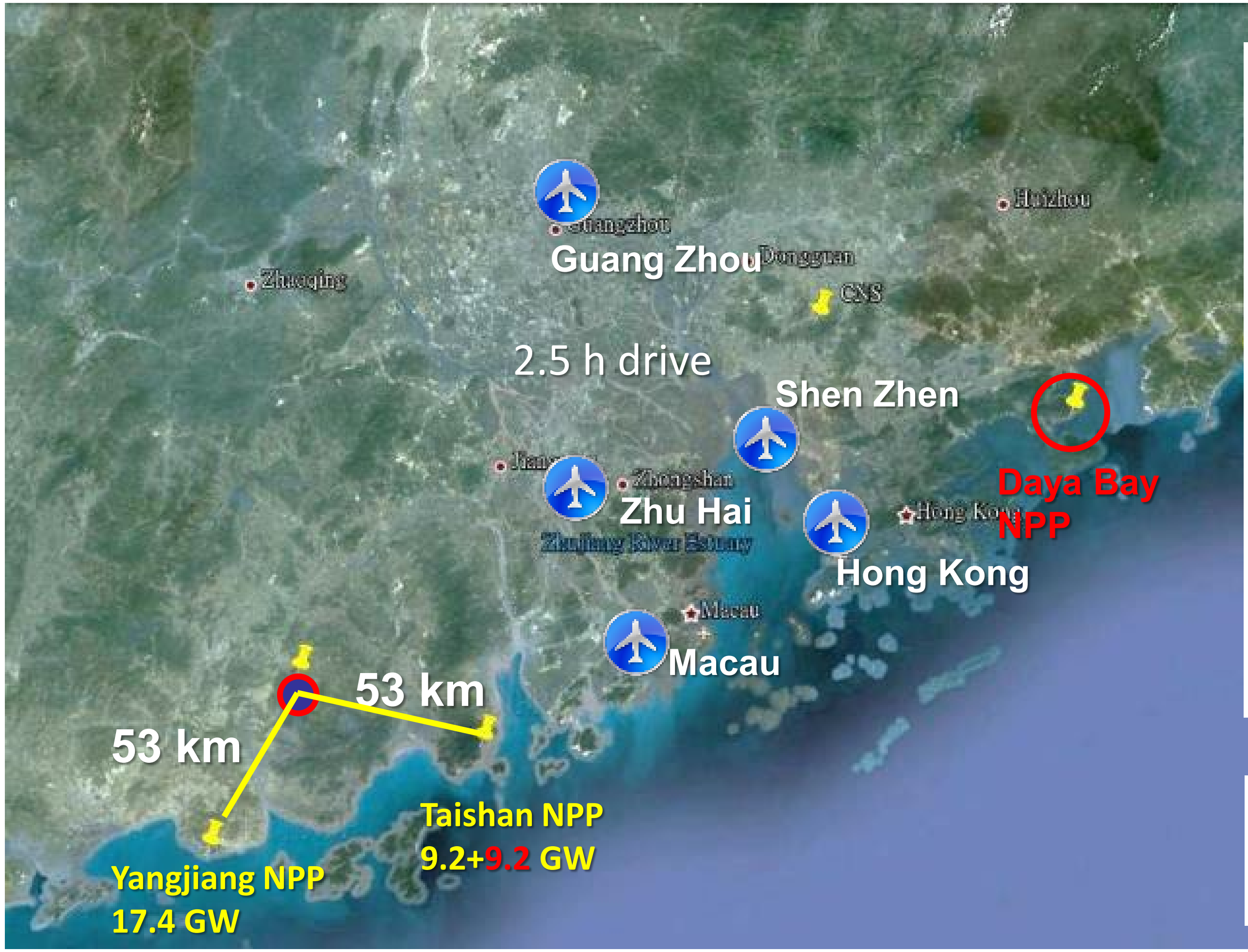

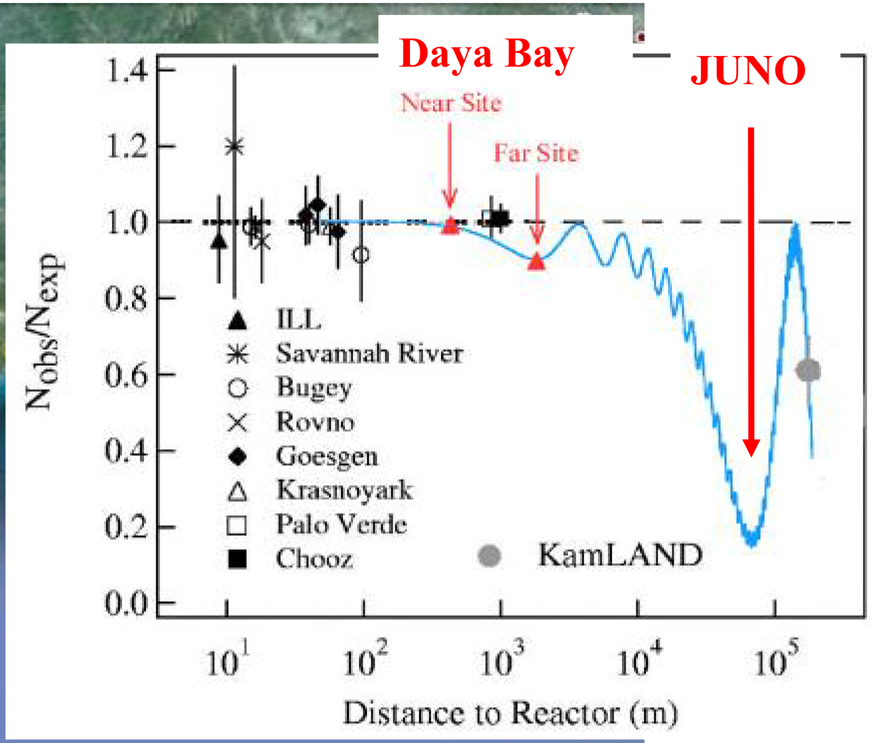

Talk by Y.F. Wang at ICFA seminar 2008, Neutel 2011;
Paper by L. Zhan, Y.F. Wang, J. Cao, L.J. Wen,
PRD78:111103,2008; PRD79:073007,2009

Reactor Neutrinos: Production and Detection

Neutrinos dominantly come from ^{235}U and ^{239}Pu
For example:

$$^{235}_{92}U + n \rightarrow X_1 + X_2 + 2n$$

$$^{94}_{40}Zr \qquad ^{140}_{58}Ce$$

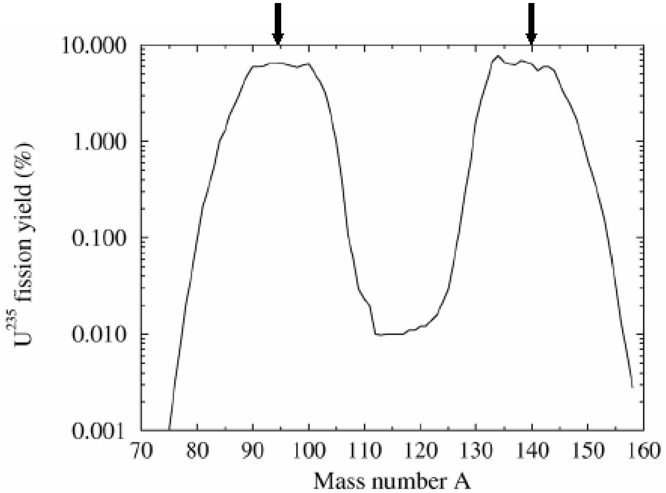

Signal: Inverse beta-decay (IBD) events

$$\bar{\nu}_e + p \rightarrow e^+ + n$$

$\tau \approx 200\mu s$

n + p → d + γ (2.2 MeV)

Prompt (e^+) and delayed(nH) coincidence in time, space with distinct energy features

Proton source: Liquid Scintillator (LS, C_nH_{2n+2}) :

- Proton rich material (highest per volume)
- Target and detector at the same time
- High light yield, fast, well understood
- Easy handling for very large volume
- Cheap, only second to water

Each fission generates ~6 neutrinos → 6 ×10^{20} /s/reactor with 3 GW_{th} power

Mass Ordering by Reactor Neutrinos

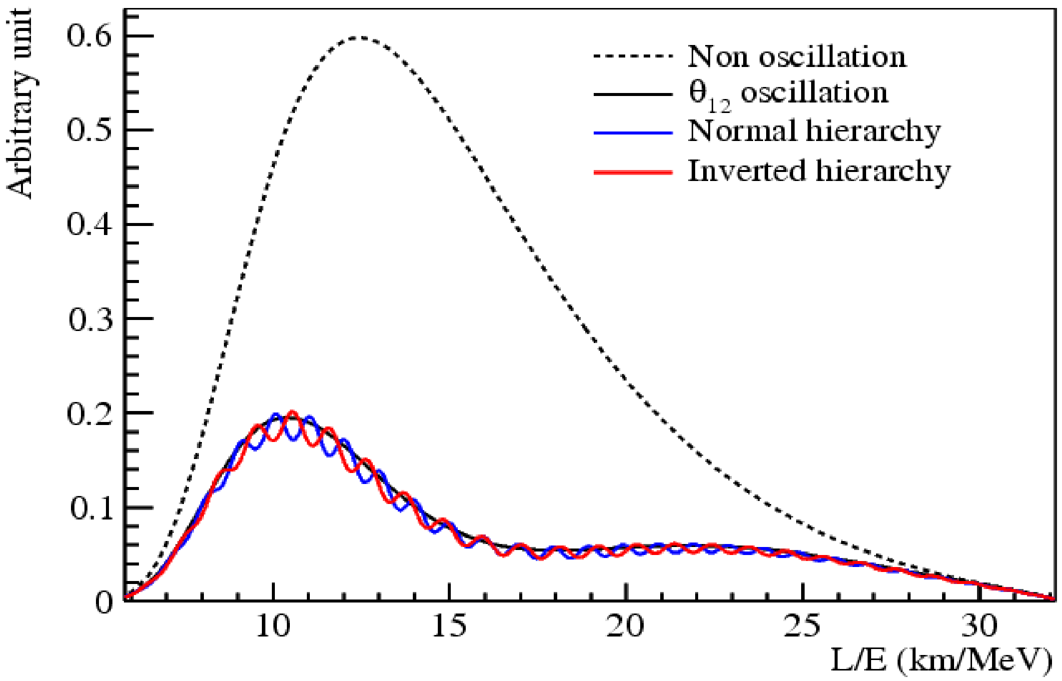

$$
\begin{aligned}
\Delta m^2_{31} &= \Delta m^2_{32} + \Delta m^2_{21} \\
\mathrm{NH}: \ |\Delta m^2_{31}| &= |\Delta m^2_{32}| + |\Delta m^2_{21}| \\
\mathrm{IH}: \ |\Delta m^2_{31}| &= |\Delta m^2_{32}| - |\Delta m^2_{21}|
\end{aligned}
$$

$$\frac{\Delta m^2_{21}}{|\Delta m^2_{31}|} \sim 3\%$$

- **Key parameters:**
  - Detector size: 20 kt
  - Energy resolution: 3%/√E
  - Thermal power: 36 GW
  - Baseline: ~58 km

L. Zhan, YFW et.al, PRD79:073007, 2009

$$
\begin{aligned}
P_{ee}(L/E) &= 1 - P_{21} - P_{31} - P_{32} \\
P_{21} &= \cos^4(\theta_{13}) \sin^2(2\theta_{12}) \sin^2(\Delta_{21}) \\
P_{31} &= \cos^2(\theta_{12}) \sin^2(2\theta_{13}) \sin^2(\Delta_{31}) \\
P_{32} &= \sin^2(\theta_{12}) \sin^2(2\theta_{13}) \sin^2(\Delta_{32})
\end{aligned}
$$

S. Petcov and Piai, Phys. Lett. B 553, 94-106(2002)
J. Learned et al., PRD 78(2008)071302
L. Zhan, YFW et al., PRD 78(2008)111103

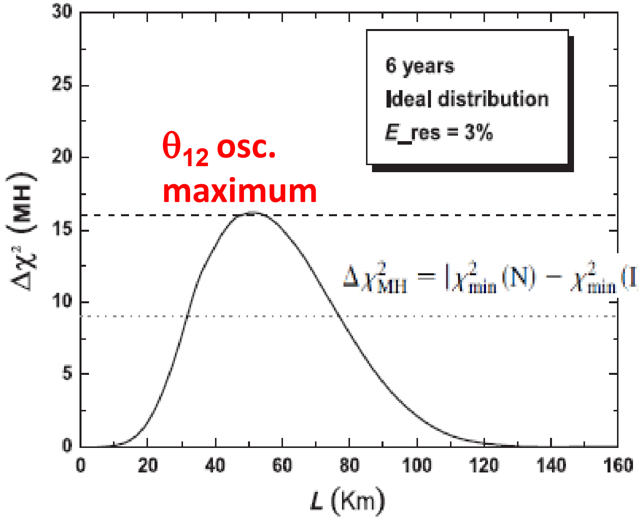

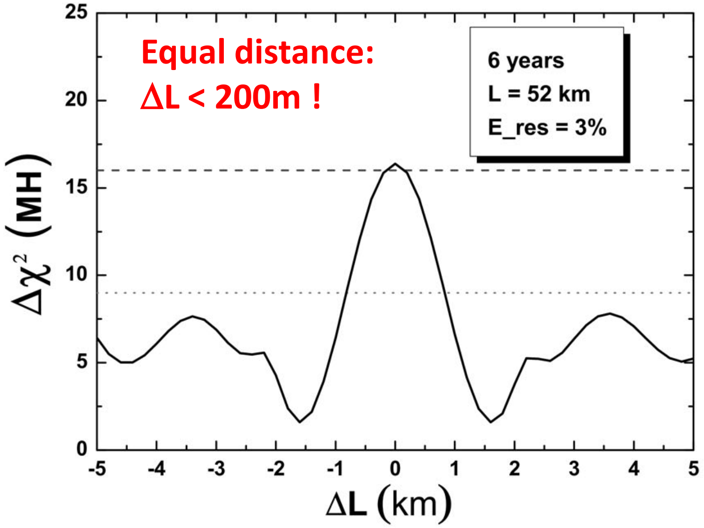

Y.F Li *et al*, PRD 88, 013008 (2013)

JUNO Project and the collaboration

- Project firstly approved in China in 2013 and later in other countries. Civil construction started in 2015
- Collaboration established in 2014, now >700 collaborators from 70 institutions in 16 countries/regions

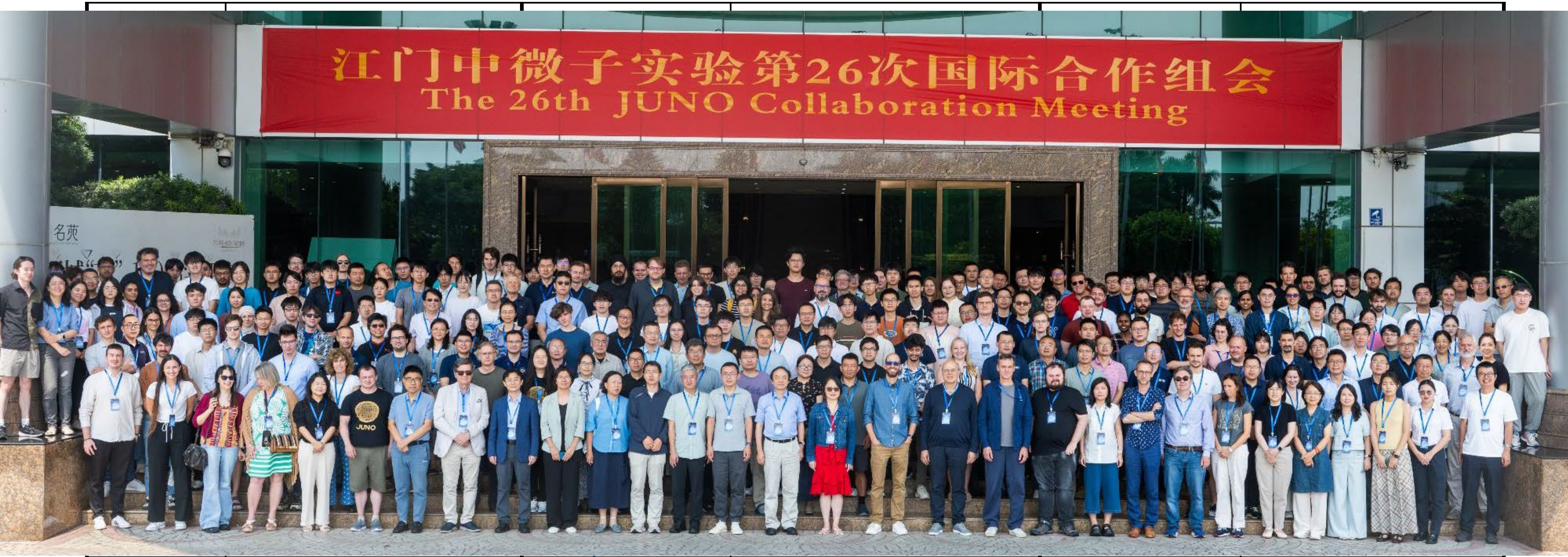

China	Nankai U.	**Germany**	U. Hamburg	**USA**	**UC-Irvine**
China	NCEPU	**Germany**	JGUMainz	**USA**	UMD-G
China	NJU	**Germany**	RWTH-AC		
China	RNCG	**Germany**	TUM		

+Observers: **USTC, Peking Uni., Jilin Uni., Beijing Normal Uni., CIAE (China), PUC, UEL (Brazil)**

JUNO Detector Design

- Target mass of 20 kt liquid scintillator ➔ × 20 KamLAND, × 70 Borexino
- Energy resolution < 3%@ 1MeV ➔ > 1200 PE/MeV

Calibration house

VETO system

- **Top Tracker: plastic scintillator**
- **Water + 2400 20'' PMT + 348 20'' spare PMTs + 600 8'' PMTs from Daya Bay**
- **Earth Magnetic Field shielding coils**

Central detector

- **Steel structure**
- **Acrylic sphere + 20kt Liquid scintillator**
- **17612 20'' PMT + 25600 3'' PMT**

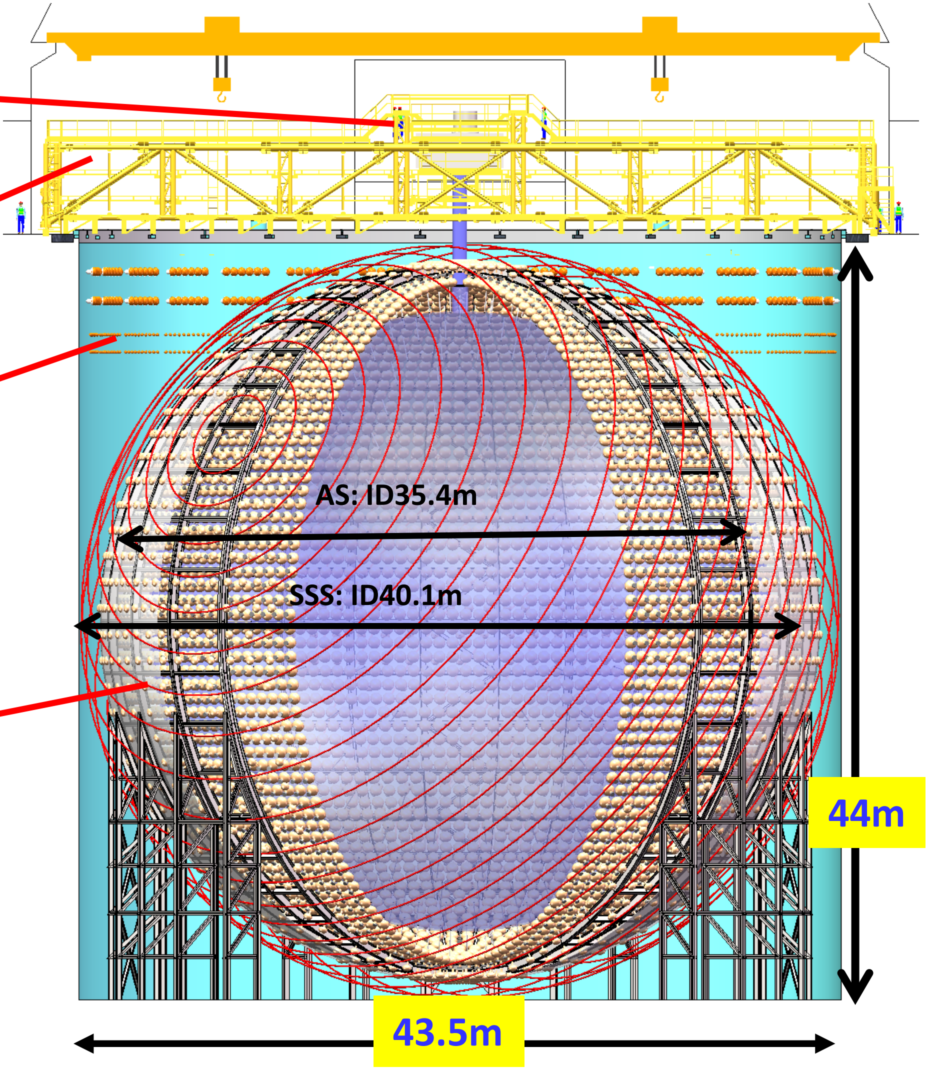

	KamLAND	JUNO	Ratio
Photon Statistics	**250 p.e./MeV**	**1200 p.e./MeV**	**5**
PMT coverage	**34%**	**75%**	**2.2**
LS transparency	**~12 m**	**> 20 m**	**~0.9**
Light yield (anthracene)	**30%**	**45%**	**~1.5**
Detection Eff.(QE×CE)	**~15%**	**30%**	**~ 2**

Main technical challenges

- ➢ Precise mechanical structure for small clearance between PMTs
- ➢ Very transparent LS
- ➢ High photon eff. PMTs

arXiv:1508.07166

Prog. Part. Nucl. Phys. 123(2022), 103927

Central Detector

- SS structure to hold the acrylic tank and PMTs, through steel bars with springs and rotating heads
- Stress sensors on steel bars
- Clearance between PMTs is ~3 mm, to maximize coverage
- 263 Acrylic panels thermally pressed and machined to the spherical shape, bonded together in-situ through PMMA polymerization
  - Stress on acrylic < 3.5 MPa
  - Difference of thermal expansion requires ±5 °C since construction

Eur.Phys.J.Plus 139 (2024) 12, 1128, arXiv: 2311.17314

PMTs and Electronics

	LPMT (20-inch)		SPMT (3-inch)
	Hamamatsu	NNVT	HZC
Quantity	5000	15012	25600
Charge Collection	Dynode	MCP	Dynode
Photon Efficiency	28.5%	30.1%	25%
Dynamic range	[0, 100] PEs		[0, 2] PEs
Coverage	75%		3%
Reference	Eur.Phys.J.C 82 (2022) 12, 1168		NIM.A 1005 (2021) 165347

LPMT & sPMT

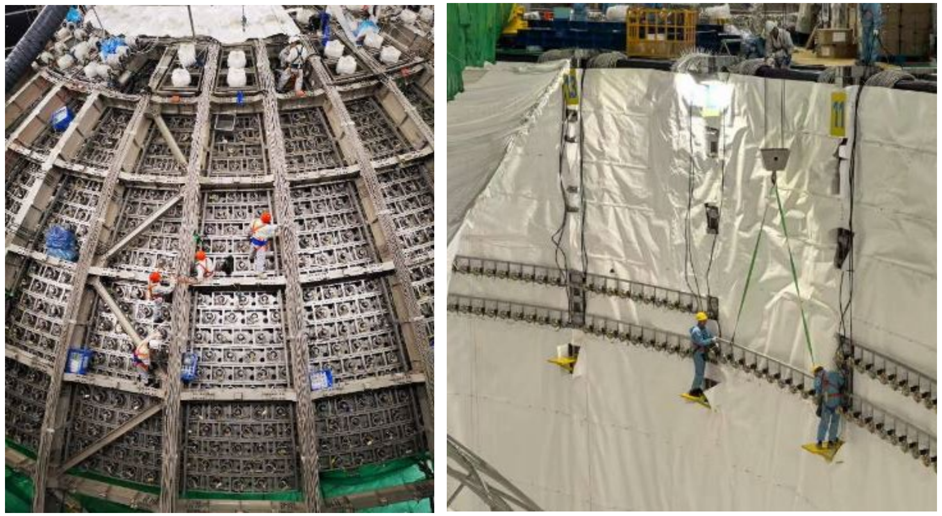

PMT and Underwater box installation

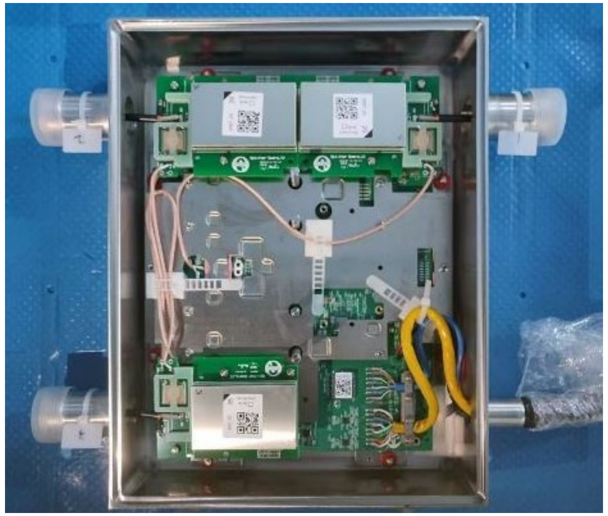

LPMT Underwater box

sPMT Underwater box

Liquid Scintillator

Posters: 324, 373, 171, 363, 337

◆ For optimal transparency and light yield:

JUNO LS: *NIMA 988 (2021) 164823*

- ⇨ Recipe: LAB + 2.5g/L PPO + 3 mg/L bis-MSB + 0.005% BHT
- ⇨ Goal: LAB attenuation length > 24m, LS attenuation length > 20m, U/Th ~ 10^{-17} g/g
- ⇨ Production: Four purification plants + LS Mixing + QA/QC + high purity N_2 and water

5000 m^3 LAB storage tank

1) Al_2O_3 for optical transparency

2) Distillation for radiopurity

Mix LAB with PPO, bis-MSB and BHT

1800 m SS pipes to underground

3) Water extraction to remove radioactive impurities

4) Gas stripping to remove Rn and O_2

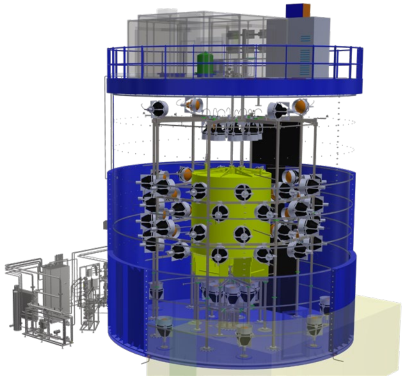

OSIRIS to monitor Rn and other backgrounds

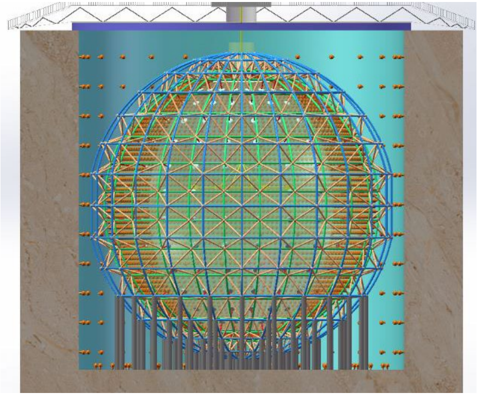

Background Control before the Liquid Filling

- U/Th/^{40}K in raw materials:
  - Steel <1 ppb, raw LAB <1 ppq, PPO <0.1 ppt, Bis-MSB <3 ppt, BHT <0.2 ppt, acrylic <1ppt, water <0.1-1.0 ppq
- Water:
  - Resistivity~18 MΩ*cm, U/Th $< 10^{-15}$ g/g, Rn < 10mBq/m^3

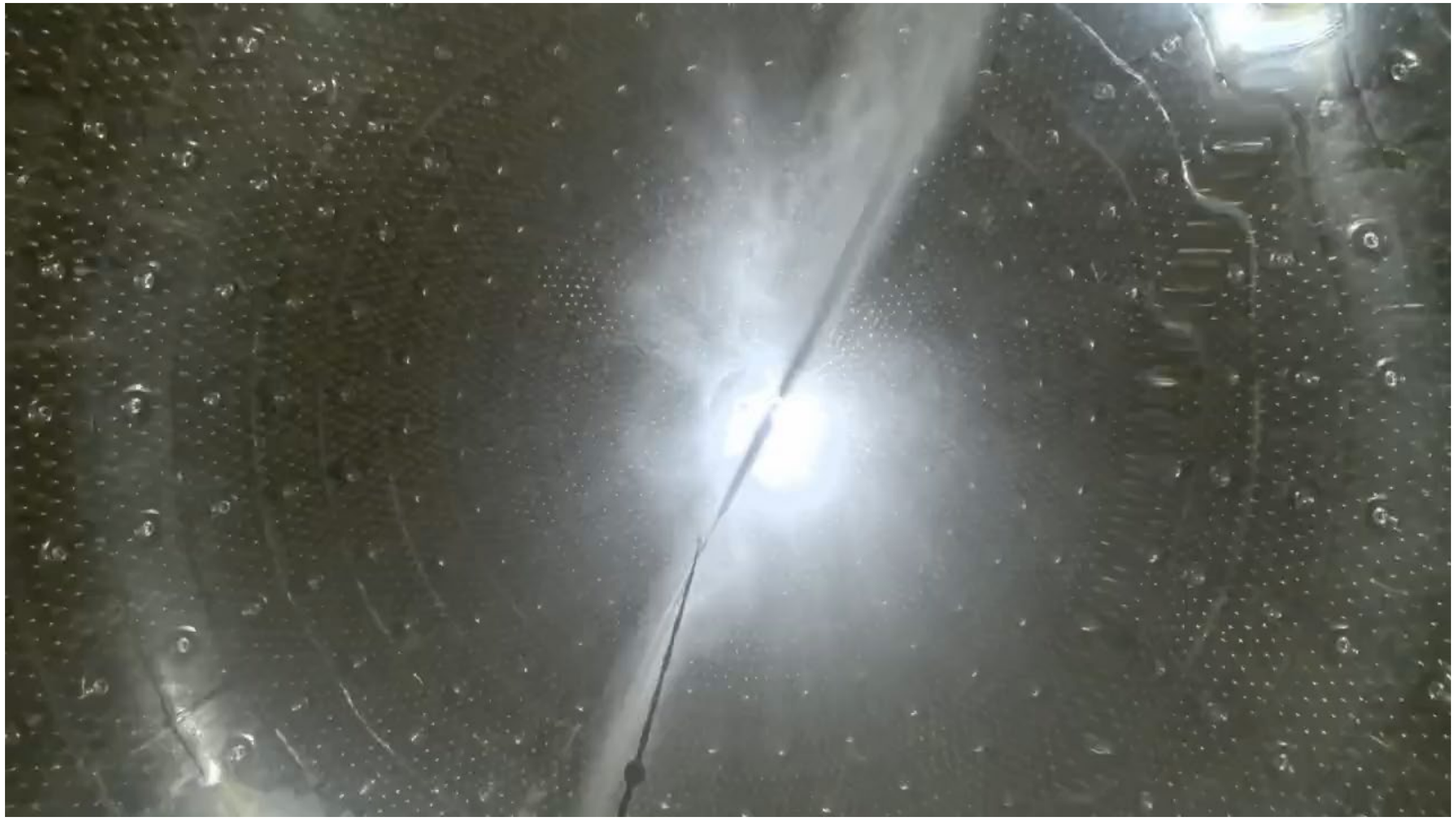

Water soluble paper film on acrylic to stop Rn decay daughters

- Surface protection and cleaning, clean room and air dust removal, …
- Air tight by leak check:
  - < 1 mBq/m^3 ^{222}Rn in fresh LS
- Surface cleanness:
  - Pure water wash to remove dust and paper film
  - Water filling before LS

Water and LS Filling

Posters 17， 324

- Water filling for cleaning the CD, testing the mechanical structure, as well as the detector commissioning
- Replace water by LS at a rate of 7 t/h, 6 months/volume
- Optical transparency and radioactive background control:
  - ✓ Weighted average LS attenuation length > 20m
  - ✓ Weekly LAB/LS sampling: U/Th < 1×10^{-16} g/g by ICP-MS
  - ✓ ^{222}Rn in fresh LS by OSIRIS+CD: < 1 mBq/m^3
  - ✓ ^{14}C ~$(4\text{-}5)\times10^{-17}$ g/g measured by several methods

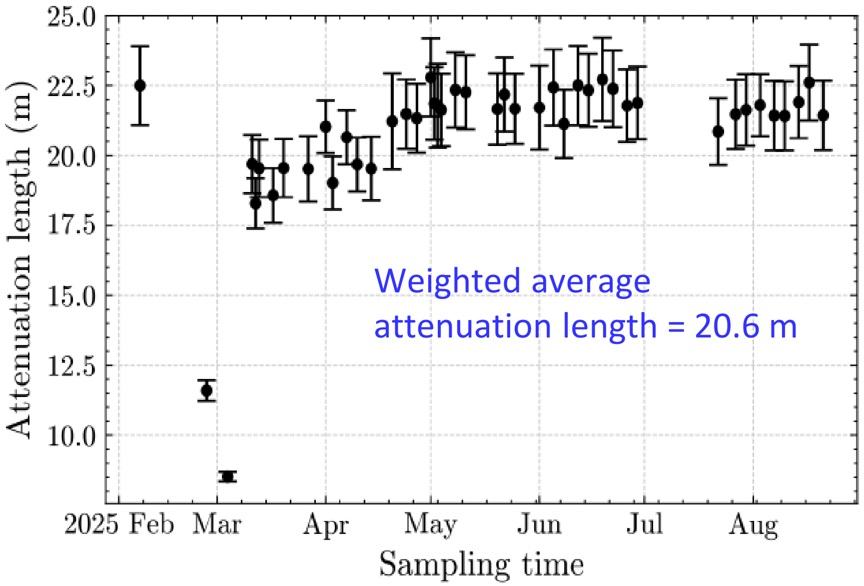

Weighted average attenuation length = 20.6 m

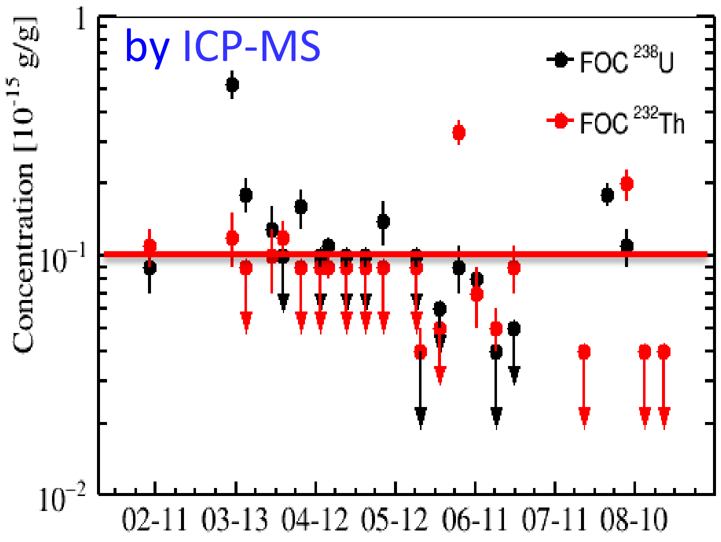

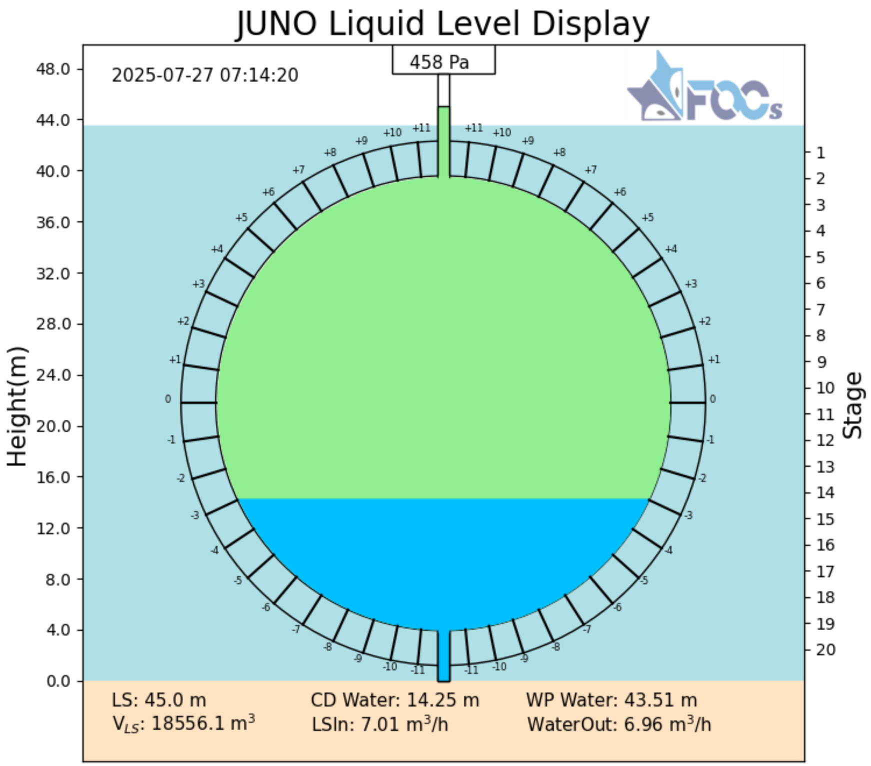

- ➢ LS Filling completed on 8/22/2025
- ➢ LS in the CD: 23231.6 m^3
- ➢ Water in the pool: 41225.1 m^3

Performance of the Detector

PMTs, Electronics and Trigger

Posters: 218, 220, 347, 340, 370

- Large PMTs
  - 17612-16 LPMTs installed for CD, 2400-1 LPMTs installed for VETO
  - ~26 dead PMTs + electronics, ~1.2/month
  - ~600 flashing PMTs (turned off)
  - Gains of MCP (Dynode) PMTs are reduced from 7.4×10^6 to 4.0×10^6 (6.5×10^6 to 5.5×10^6), efficiencies not affected
- Noise of electronics for LPMTs:
  - Stable pedestals
  - RMS ~2.8 ADC ch. ➔ ~0.055 PE
  - PMT threshold: 0.2-0.3 PE
- Dark rate continuously decreasing
- sPMTs have similar performance
- Trigger threshold: ~200 keV

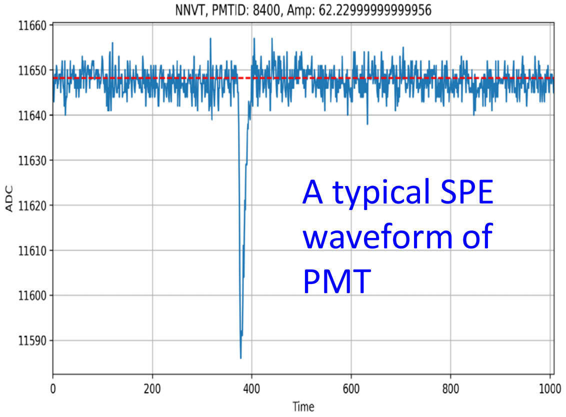

A typical SPE waveform of PMT

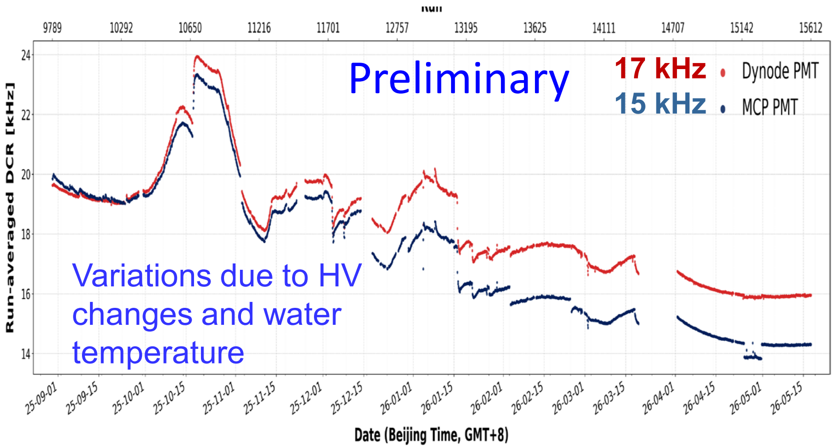

Variations due to HV changes and water temperature

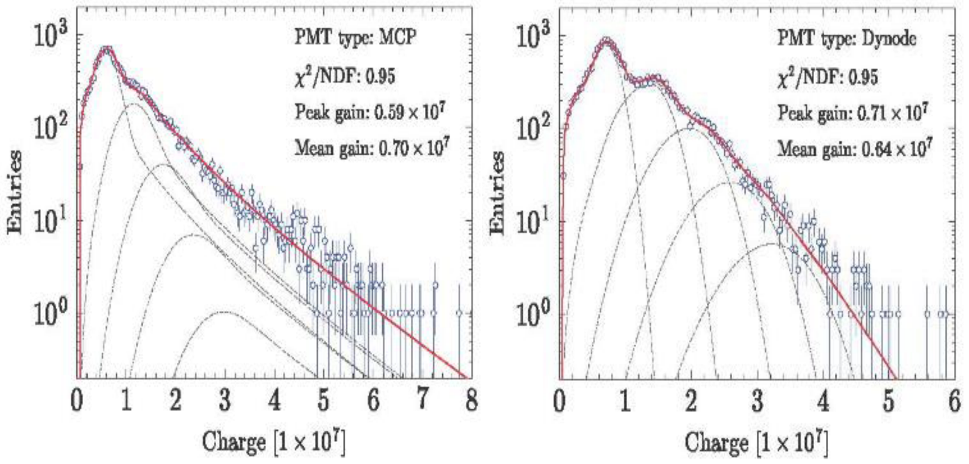

SPE pulse shape and calibration

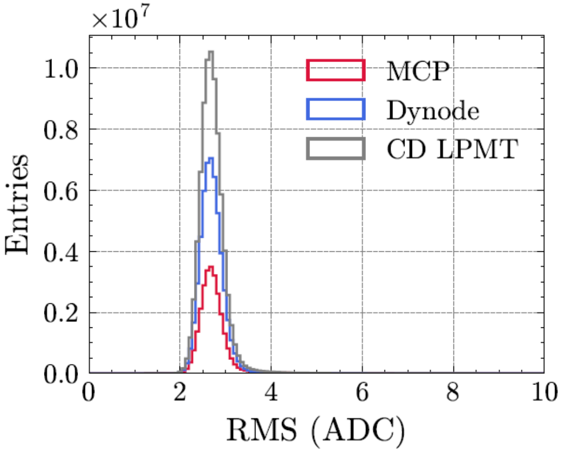

Noise of Electronics noise

Backgrounds of the Detector

Poster: 344

- For reactor neutrinos: (r < 17.2m & E > 0.7MeV)
  - ⇨ Clearly see the steel structure: acrylic surface background from dust is limited ➔ washing is effective
  - ⇨ Single event rate: < 6 Hz (design 7.2 Hz)
  - ⇨ Background simulation includes LS, PMTs, steel structure, acrylic and water (including Rn) ➔ Good agreement with data
- LS purity:

Fiducial volume	^{238}U [10^{-17} g/g]	^{232}Th [10^{-17} g/g]	^{210}Po [10^4 cpd/kt]	
			Initial	Present (Jun. 1)
r < 16.5 m	8.22±0.03 ±0.68	7.8±0.1 ±0.4	4.80±0.02 ±0.14	2.25±0.01 ±0.07
r < 15.0 m	7.79±0.03 ±0.70	7.8±0.2 ±0.4	4.78±0.02 ±0.14	2.28±0.01 ±0.07

First error is statistical and the second systematic.

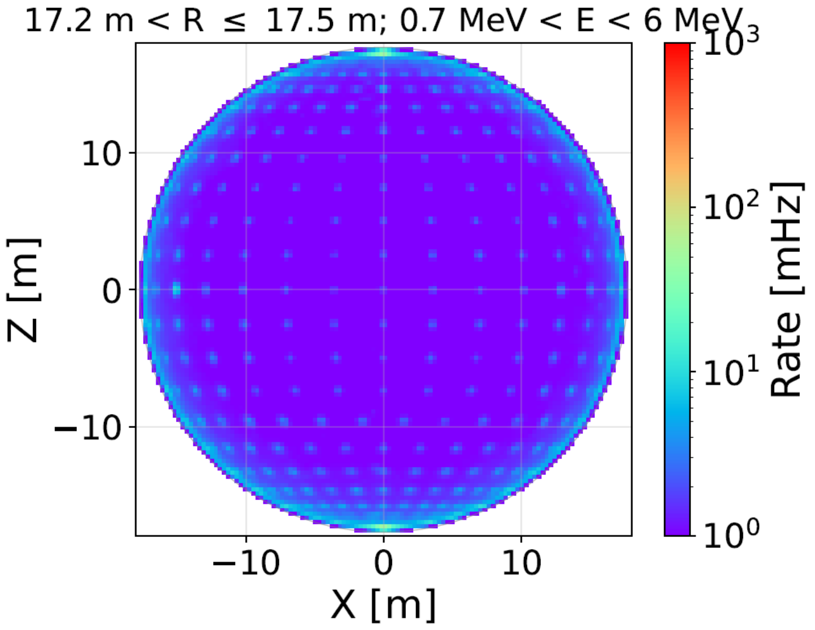

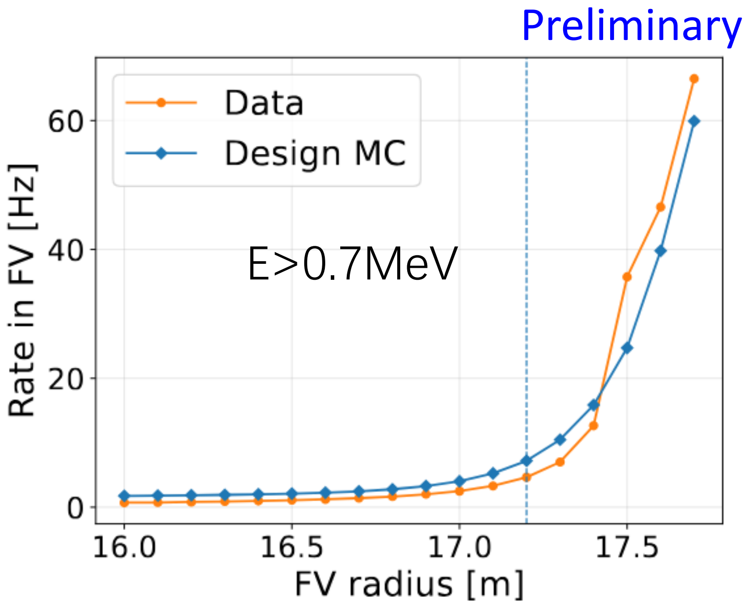

Muon Events and Track Reconstruction

Posters: 128, 283, 325

- Muon trigger rate in CD ~5 Hz, in Water Pool ~4 Hz
- Muon detection efficiency of CD through-going muons > 99.5%
- Two types of track reconstruction methods: traditional and data-driven ML
- Reconstructed angular distributions in good agreement with Monte Carlo simulation:
  - ⇨ Extremely important to veto muon tracks to reject cosmogenic ^{8}He/^{9}Li background

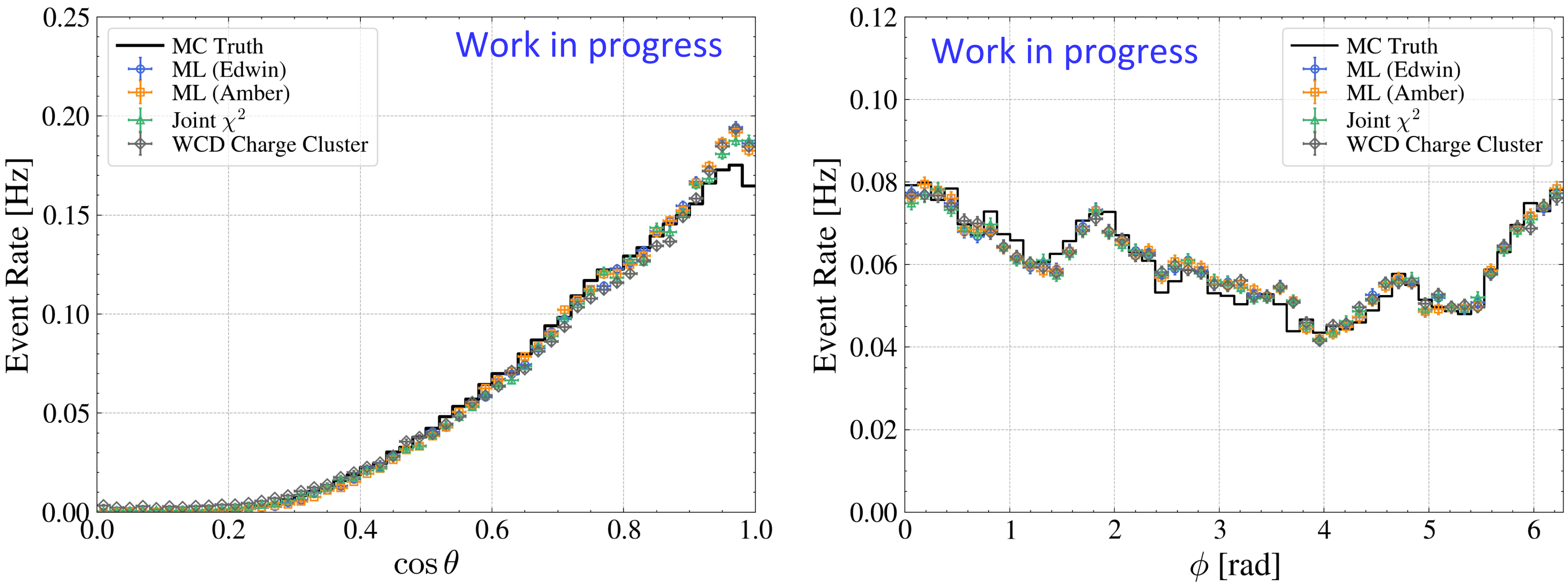

Muon's flux and energy spectrum, mountain's profile and density are well understood.

Data Taking

Posters: 338, 48, 354, 343, 254, 359

- Data taking period for this analysis: 2025.08.30-2026.05.18
- Golden data are selected for physics analysis

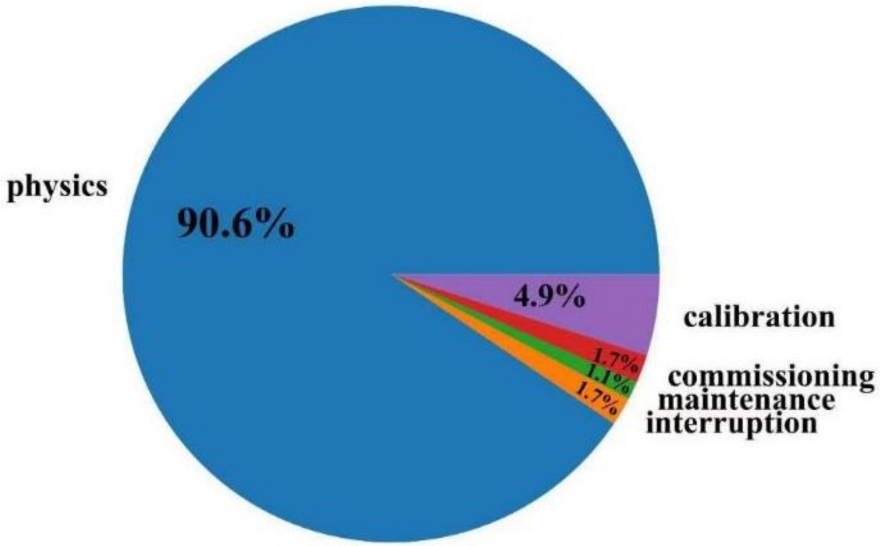

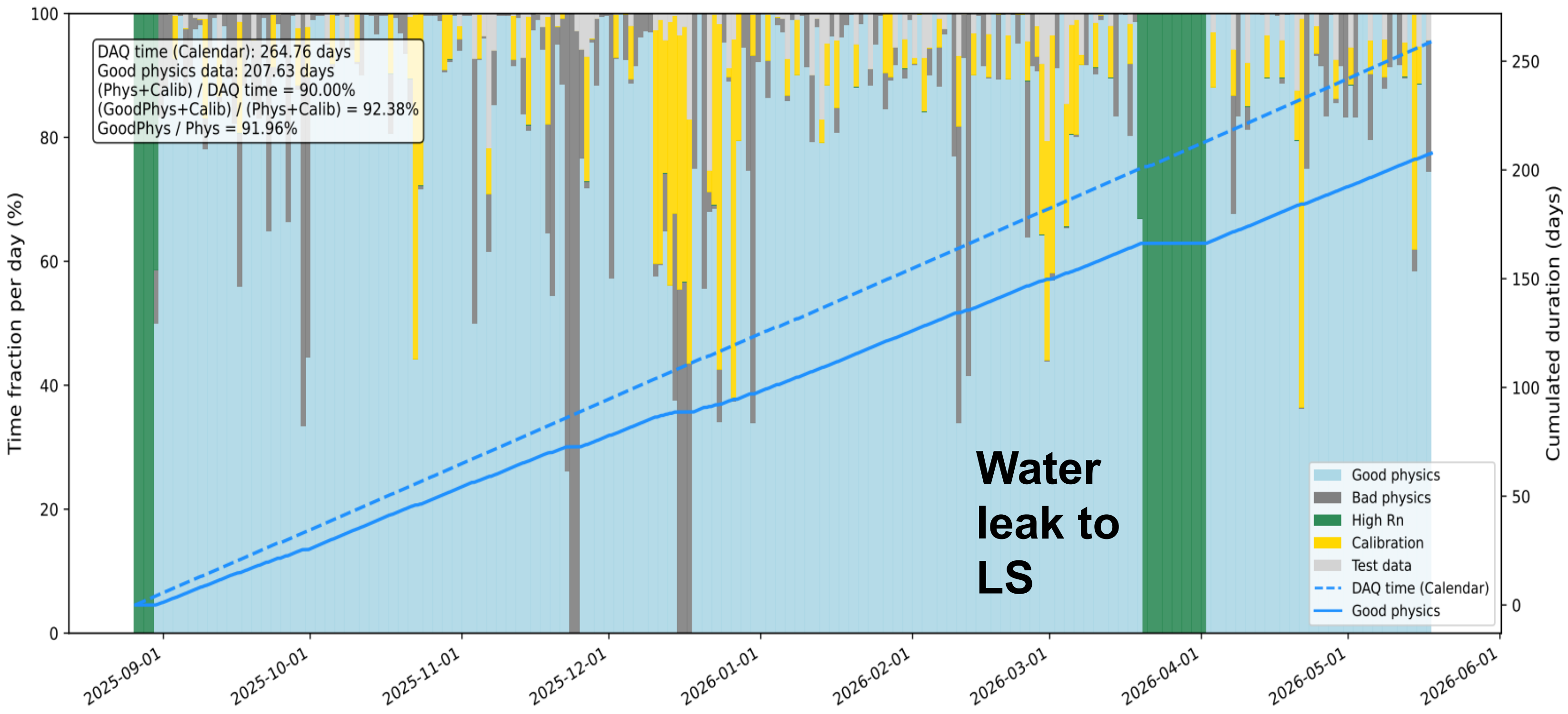

- Power outage due to weather is one of the main causes of interruptions

Cracks on the Acrylic Tank

- Main structure is safe, stress within expectations
- However, a LS leak to water happened on March 21, 2025:
  - ⇨ Abnormal trigger rate observed and confirmed by under water robot
  - ⇨ Leak was stopped within 1 week using epoxy and tape by divers
  - ⇨ Further repair by epoxy and acrylic plate to reduce the stress (pulling open the crack) by 50%
- Another leak of water to LS happened on March 19, 2026:
  - ⇨ Experienced divers were called to stop the leak within 2 days
  - ⇨ Further repair in the following two days
  - ⇨ A total of ~1Bq ^{222}Rn went into LS, 13 days of data excluded
  - ⇨ No other increase of radioactive backgrounds in LS

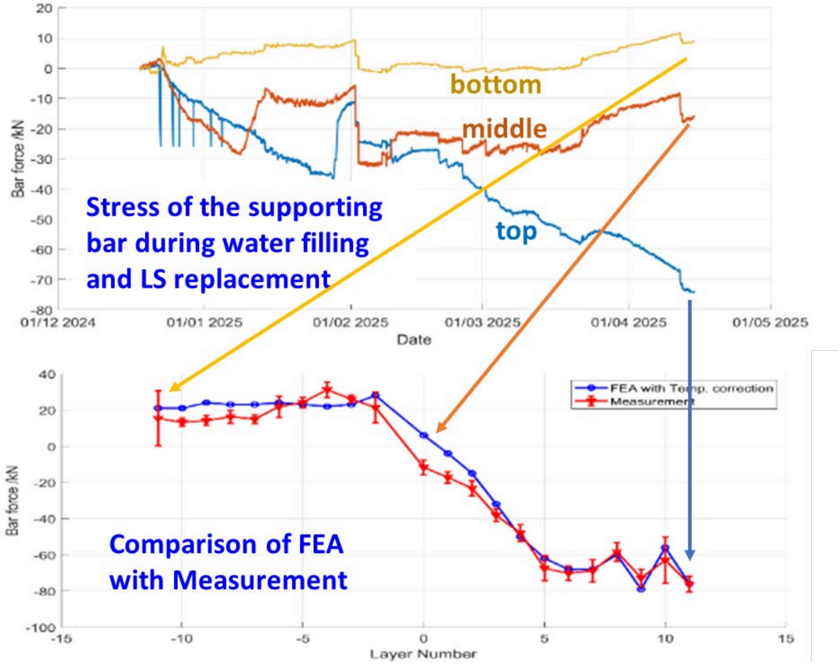

Stress of the supporting bar during water filling and LS replacement

Comparison of FEA with Measurement

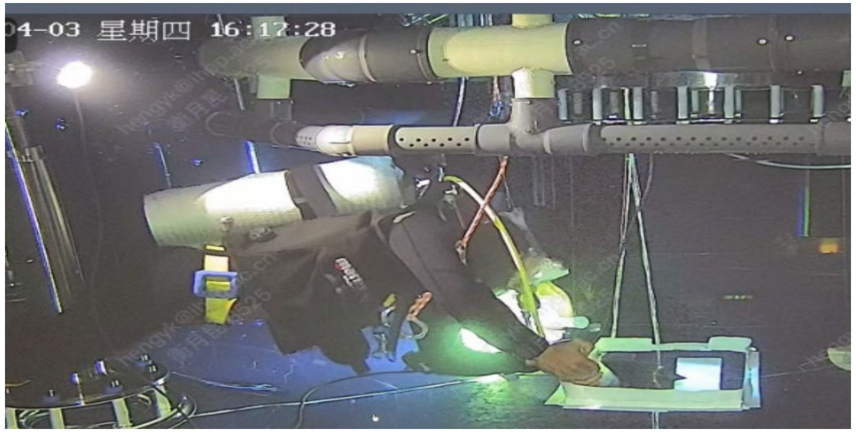

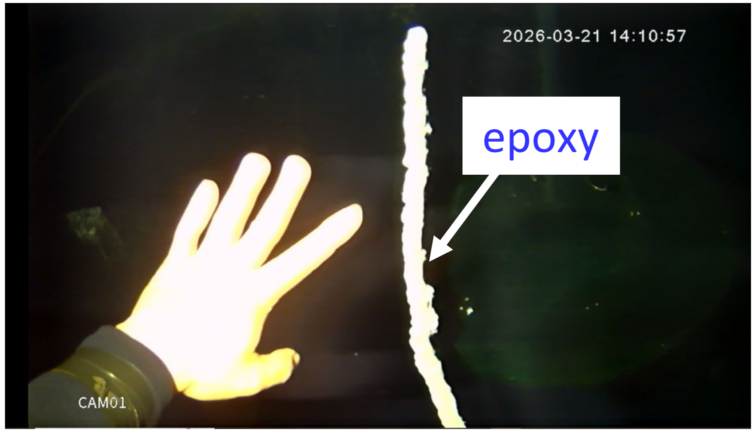

Calibration

Posters: 248, 249, 347, 340, 335

- 1D (central axis): ^{137}Cs, ^{54}Mn, ^{40}K, ^{68}Ge, ^{60}Co, Am-C, Am-Be, sensors, laser
- 2D (cable loop): Am-C, ^{68}Ge, ^{137}Cs
- 3D using cosmogenic backgrounds:
  - ⇨ Bi-Po214 from Rn decays, spallation neutrons, other cosmogenic isotopes

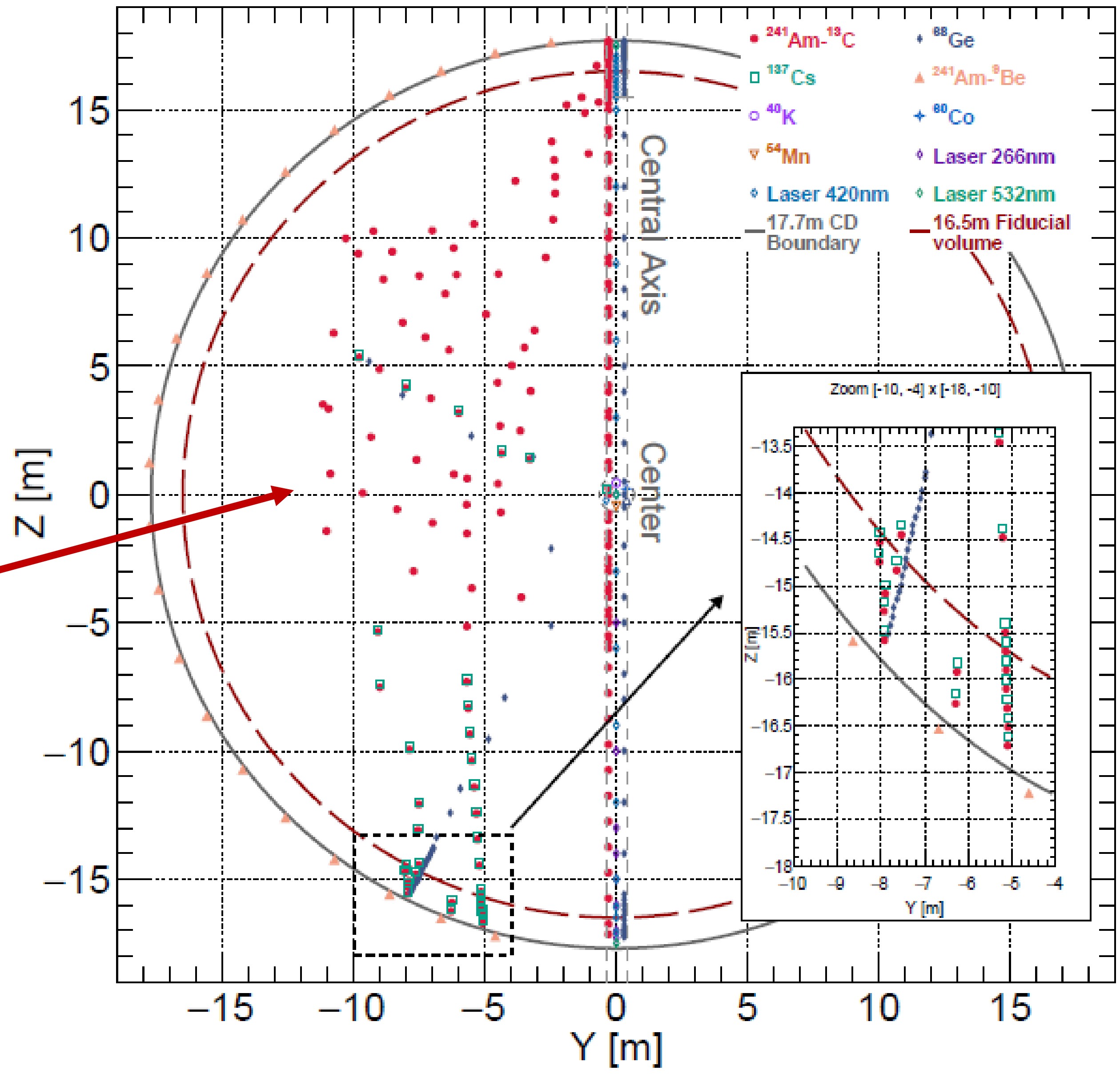

- Positions at which source calibration performed
- No ^{222}Rn leakage or other contaminations introduced during calibration

Reconstruction and Energy Correction

Posters: 419, 345, 272, 162, 323

- Vertex and energy are determined by maximum likelihood taking into account PMT response, geometry, optical properties, verified by calib. sources
- Other reconstruction methods give similar results
- Time dependent variations corrected by Po214 in the whole volume, check by n-H from IBD

Po214 - After correction

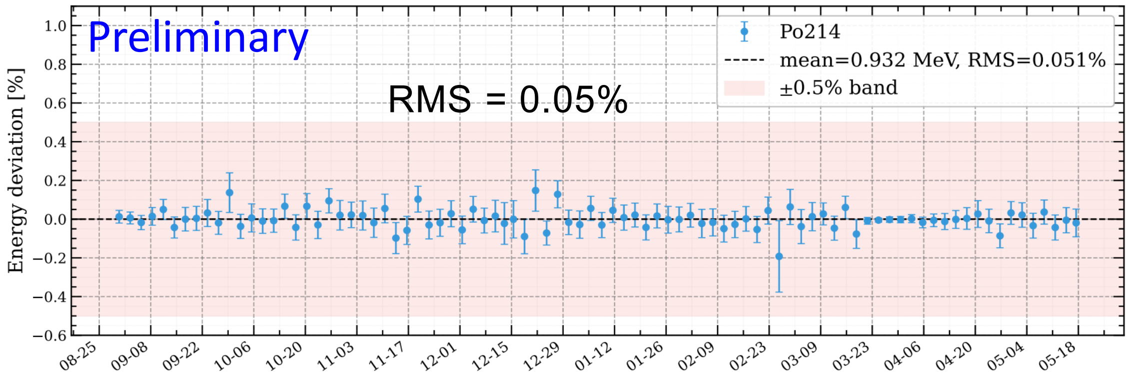

IBD nH - After correction

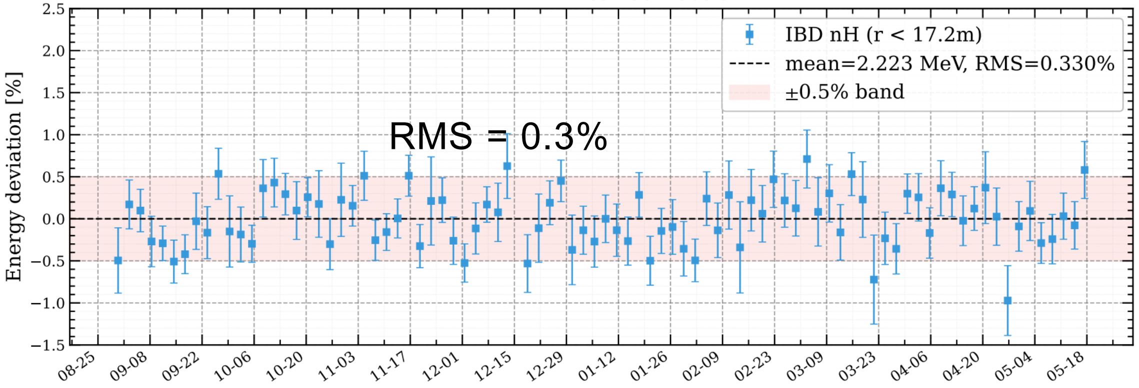

- Residual r-θ-t dependence (~1%) further corrected by ^{214}Po in the whole volume
- Energy scale anchored at nH from ^{9}Li+IBD
- Final performance checked by IBD nH in r < 17.2m
  - Residual spatial non-uniformity RMS ~0.2%
  - Residual time dependent variation RMS ~0.3%

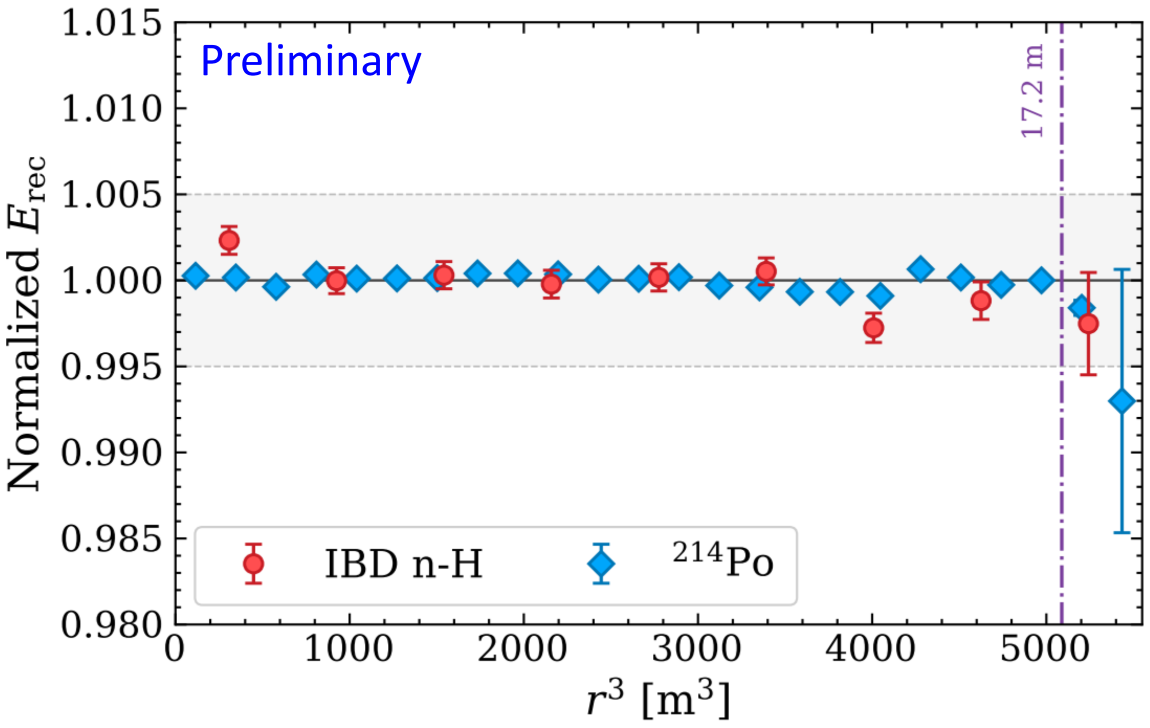

Energy Non-linearity

Posters: 334, 340,370

- Non-linearities of LS and electronics are determined by calibration sources at the center: ^{68}Ge, ^{137}Cs, ^{54}Mn, ^{40}K, ^{60}Co, Am-C, and Am-Be
- The non-linearity model for e^+ is based on Geant4 and γ-sources
- The model is constrained by cosmogenic isotopes, ^{11}C(e^+), ^{10}C(e^+), ^{12}B(e^-), ^{8}Li (e^-), ^{8}B(e^+), ^{6}He(e^-), etc. in the whole volume
- Using sPMTs to correct and constrain LPMT instrumental non-linearity
- Uncertainty < 1%

Preliminary

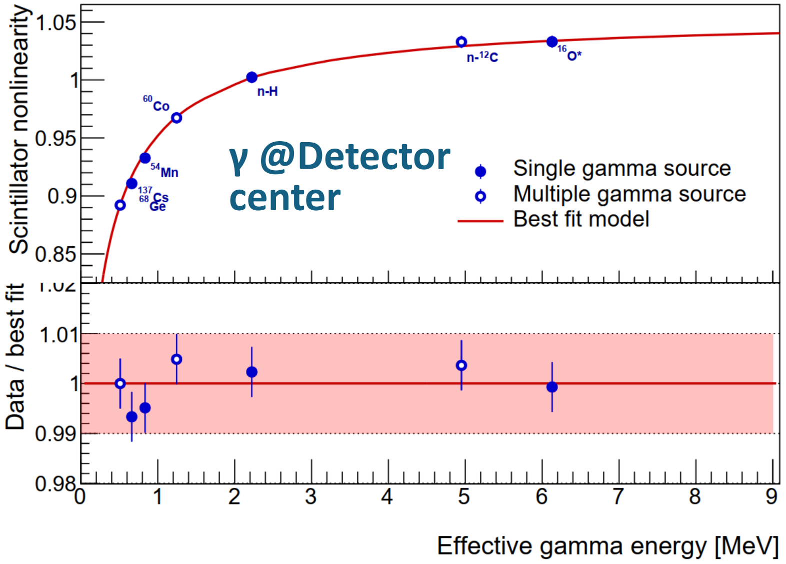

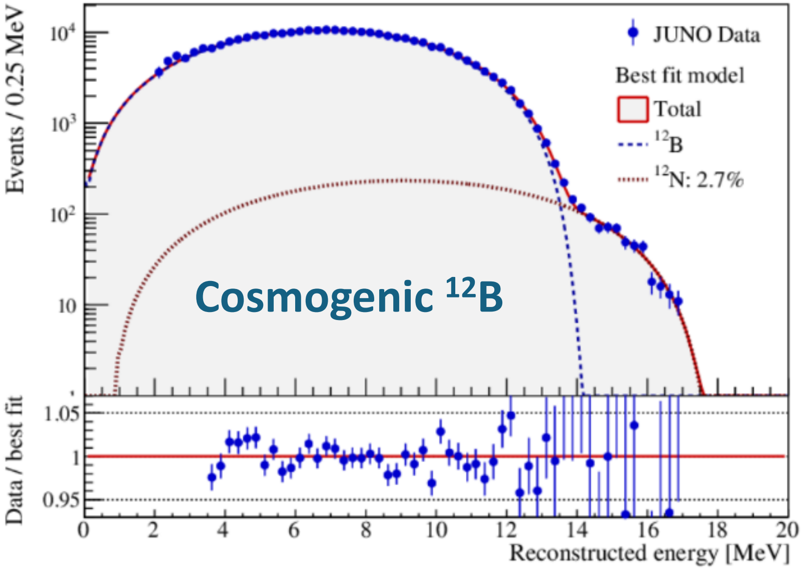

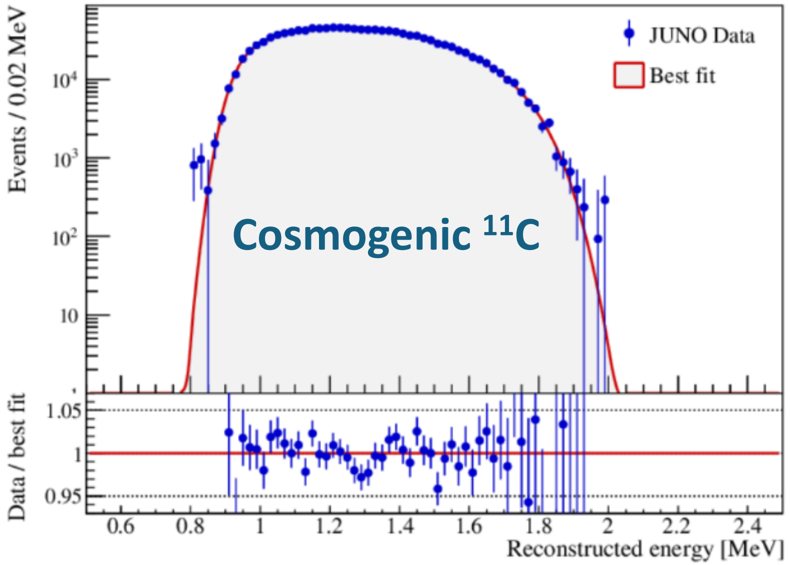

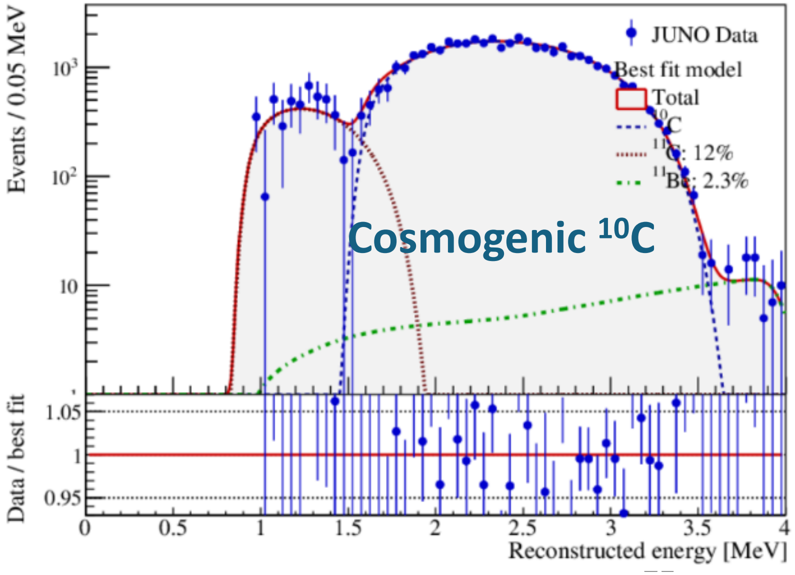

Light Yield and Energy Resolution

Posters: 270, 406

- Light yield at the detector center is ~1600 PE/MeV for ^{68}Ge and ~1785 PE/MeV for neutrons, in good agreement with MC
- Energy resolution for ^{68}Ge is ~3.5% @ 2× 0.511 MeV at the center, slightly worse than the expected 3.1%
  - ⇨ Better MC for Č process, optical boundaries, δ electrons, …
  - ⇨ Possible improvements: ML to remove ^{14}C, more calibration, better reconstruction and fitting methods, …
- Energy resolution for alpha from ^{214}Po is ~2.9% @0.93MeV

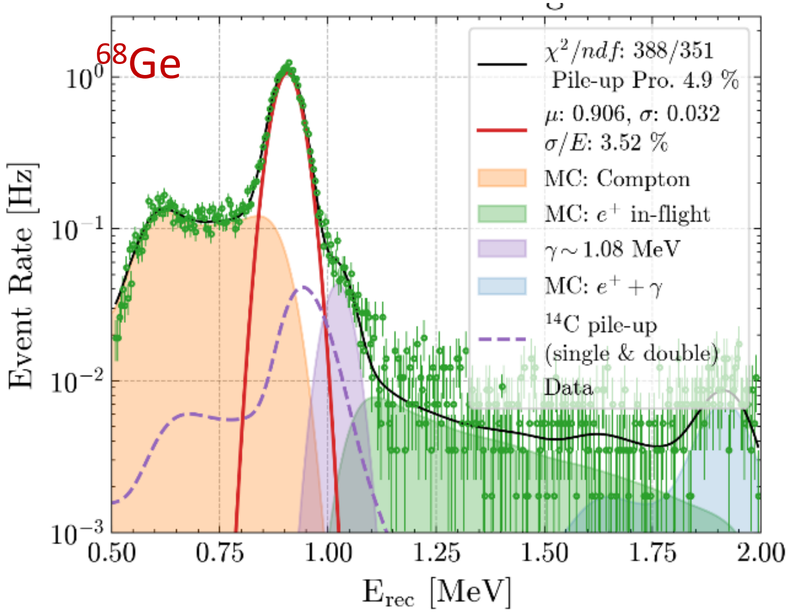

Light yield of ^{68}Ge

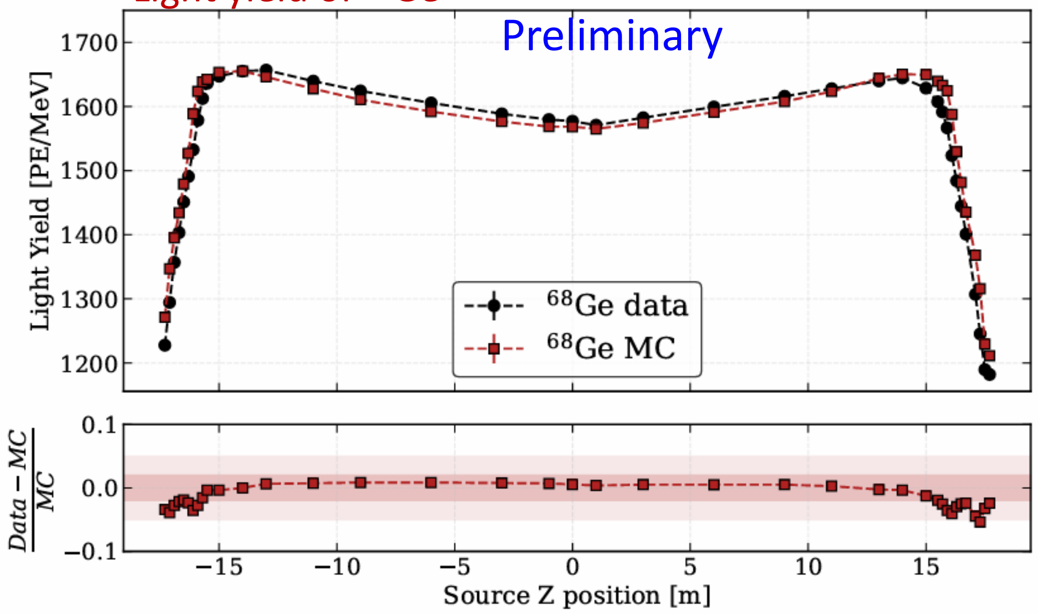

Energy resolution vs r^3

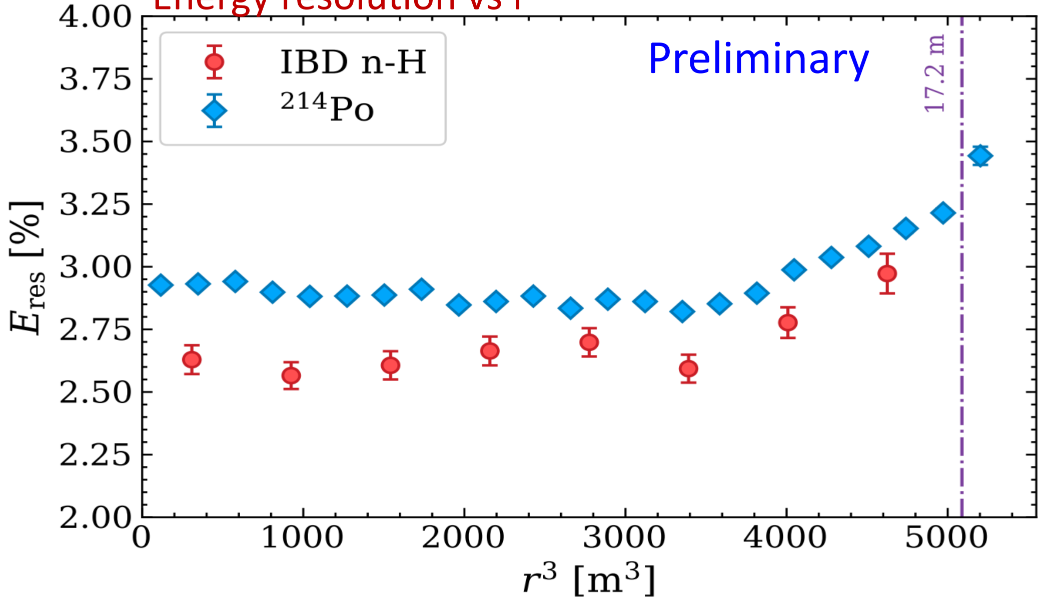

Energy Resolution Model

Poster: 406

- Energy resolution is particle type, energy and space dependent
- An analytical R-dependent resolution model for e⁺ was built using Geant4 simulation and data from calibration sources (α, γ)
- An energy response matrix was then used for e⁺ spectrum fitting after adding ^{14}C pile-up to 5% events

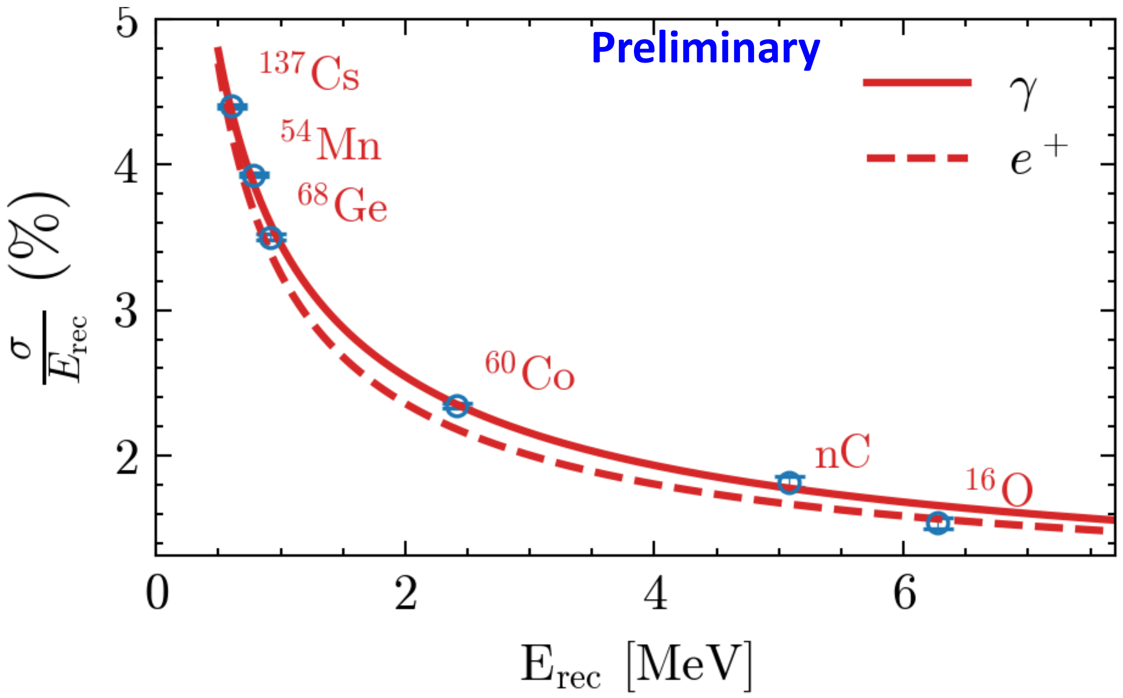

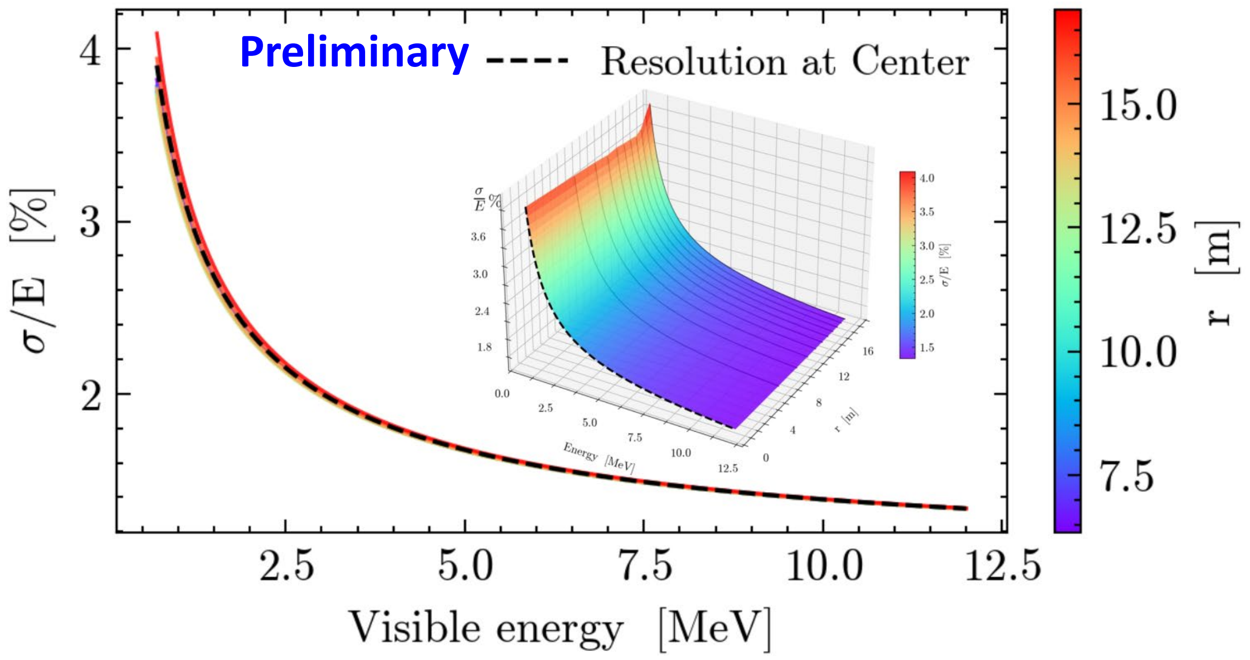

First results using 59 days of data recently published

The international journal of science / 11 June 2026

spotlight
Drug discovery

nature

FLAVOUR PROFILES

Early JUNO data capture neutrino oscillations with improved precision

Now trending
Is the hype around peptide drugs backed up by the science?

Proof of concept
How AI use might add up to success for maths and physics

Framework for life
3D structures of protein lattices in mouse egg cells

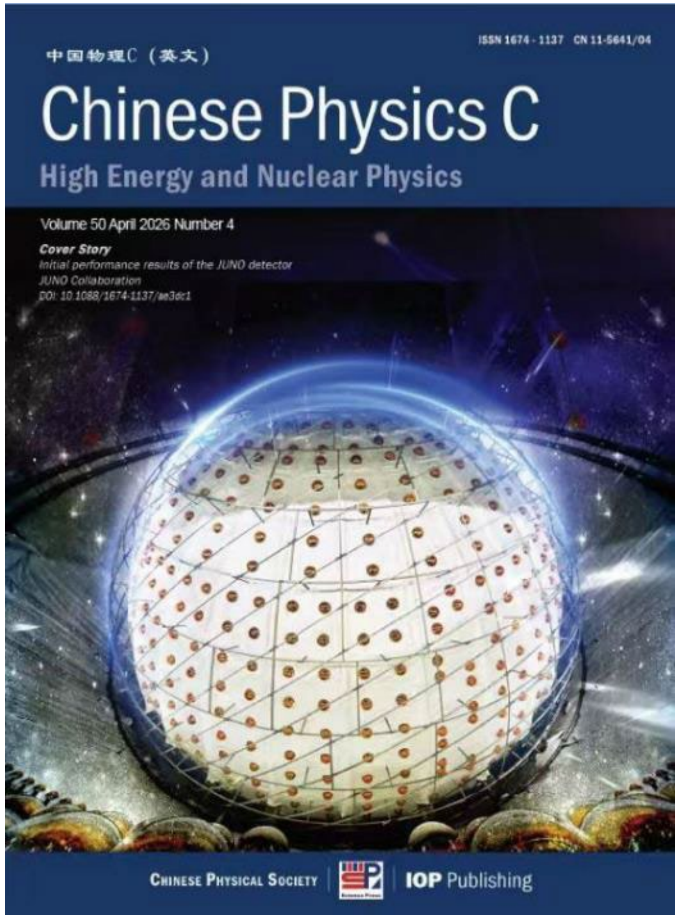

中国物理C（英文）

ISSN 1674 - 1137 CN 11-5641/04

Chinese Physics C

High Energy and Nuclear Physics

Volume 50 April 2026 Number 4

Cover Story
Initial performance results of the JUNO detector
JUNO Collaboration
DOI: 10.1088/1674-1137/ae3dc1

Chinese Physical Society IOP Publishing

Today New Results using 207 days of data

Reactor Neutrino Selection

Posters: 346, 328, 357, 273,404

- Prompt and delayed coincidence in time, space with energy features

Criterion	Selection
PMT flasher	Applied
Fiducial volume	$r_p < 17.2$ m, $\lvert z_p \rvert < 15.5$m
Prompt energy	(0.7, 12) MeV
Delayed energy	$(2.0, 2.5) \cup (4.5, 5.5)$ MeV
Coincidence time	(5, 1000) μs
Relative distance	< 1.5 m
Multiplicity cut	No other events > 0.7 MeV in the FV or (2.0, 6.0) MeV outside the FV within 2 ms before and 1 ms after the delayed event
Water pool muon veto	Veto if the delayed is within (0, 2) ms after NPE > 700 in WP
CD muon veto	Veto if the delayed is within (0, 5) ms after NPE $> 3 \times 10^4$ in CD
Spallation neutron veto	Veto if the delayed satisfies $\Delta r < 4$ m and $\Delta t < 1.2$ s after spallation neutrons with $\mathrm{NPE_{spn}} \in (3000, 30000)$ and $T_{\mathrm{spn2}\mu} \in (20, 2000)$ μs
Muon track veto	Veto if the delayed event: $\frac{\Delta r_{\mu d}}{2.5\mathrm{m}} + \frac{\Delta t_{\mu d}}{0.5\mathrm{s}} < 1$
Correlated discriminator	log(L.R.) > -1.26

Similar to our "Nature" paper

- What is new in this analysis:
  - ~10% more fiducial volume (R=16.5m➔17.2m)
  - ~60% reduction of ^{9}Li bkg.
  - a factor of 50 reduction of accidental bkg. using likelihood cut
  - model independent estimate of the ^{214}Bi bkg.

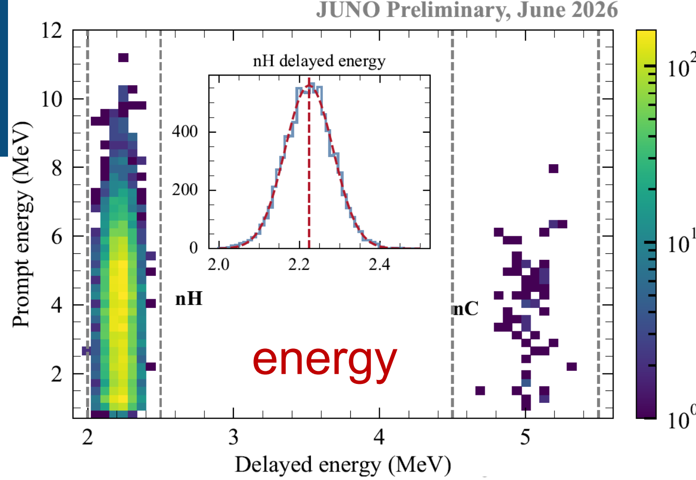

energy

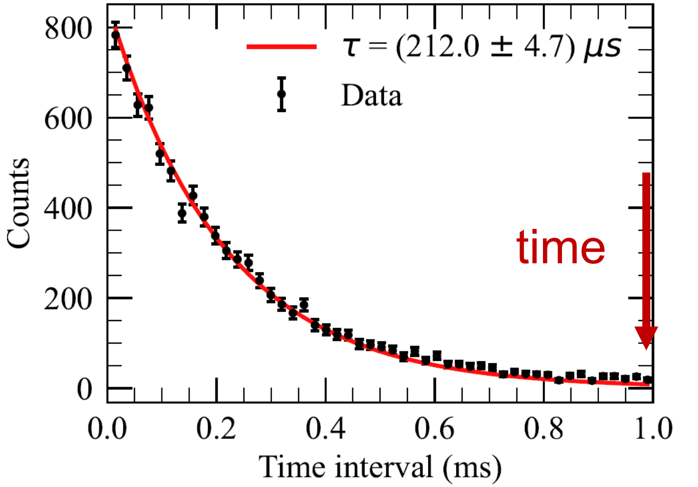

time

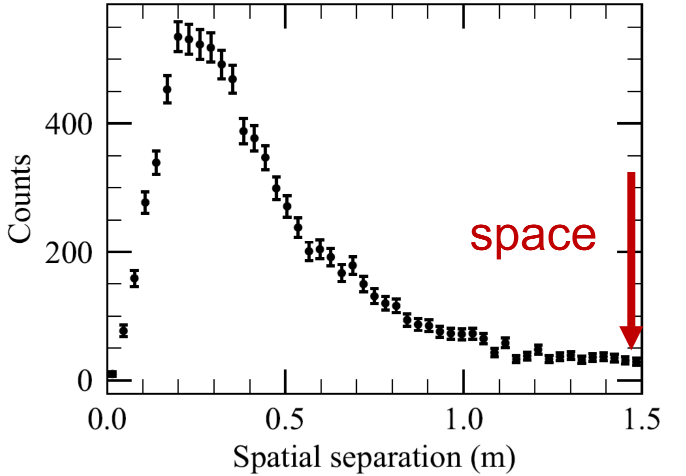

space

Reactor Neutrino Event Rate versus Time

- Measured reactor neutrino event rate consistent with expectation
- Total live time is 207.2 days

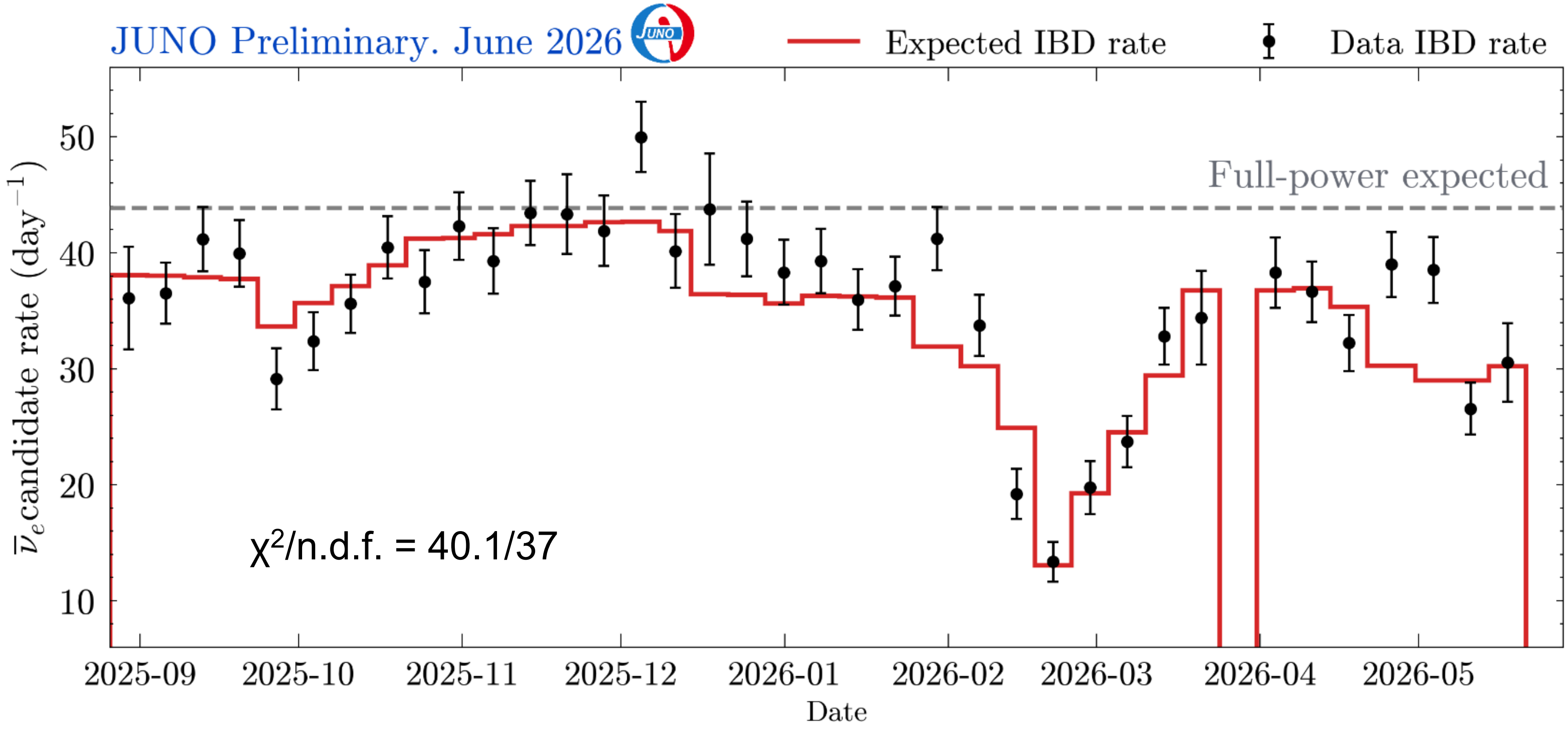

χ^2/n.d.f. = 40.1/37

Measured Reactor Neutrino Spectrum

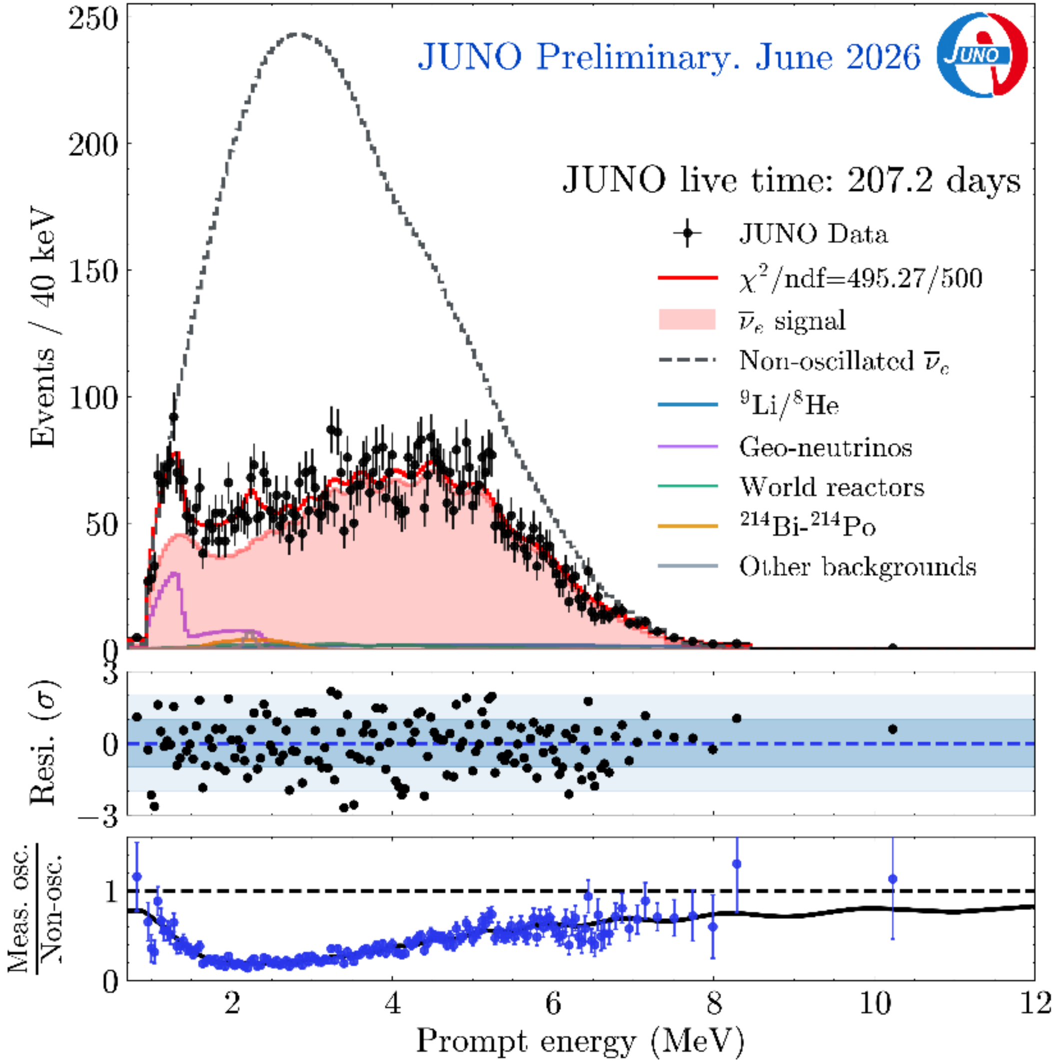

Fitting constrained by the near detector spectra from TAO (talk by Yichen) **and Daya Bay** (PRL 130 16, 161802)

Consistent results from three independent analyses

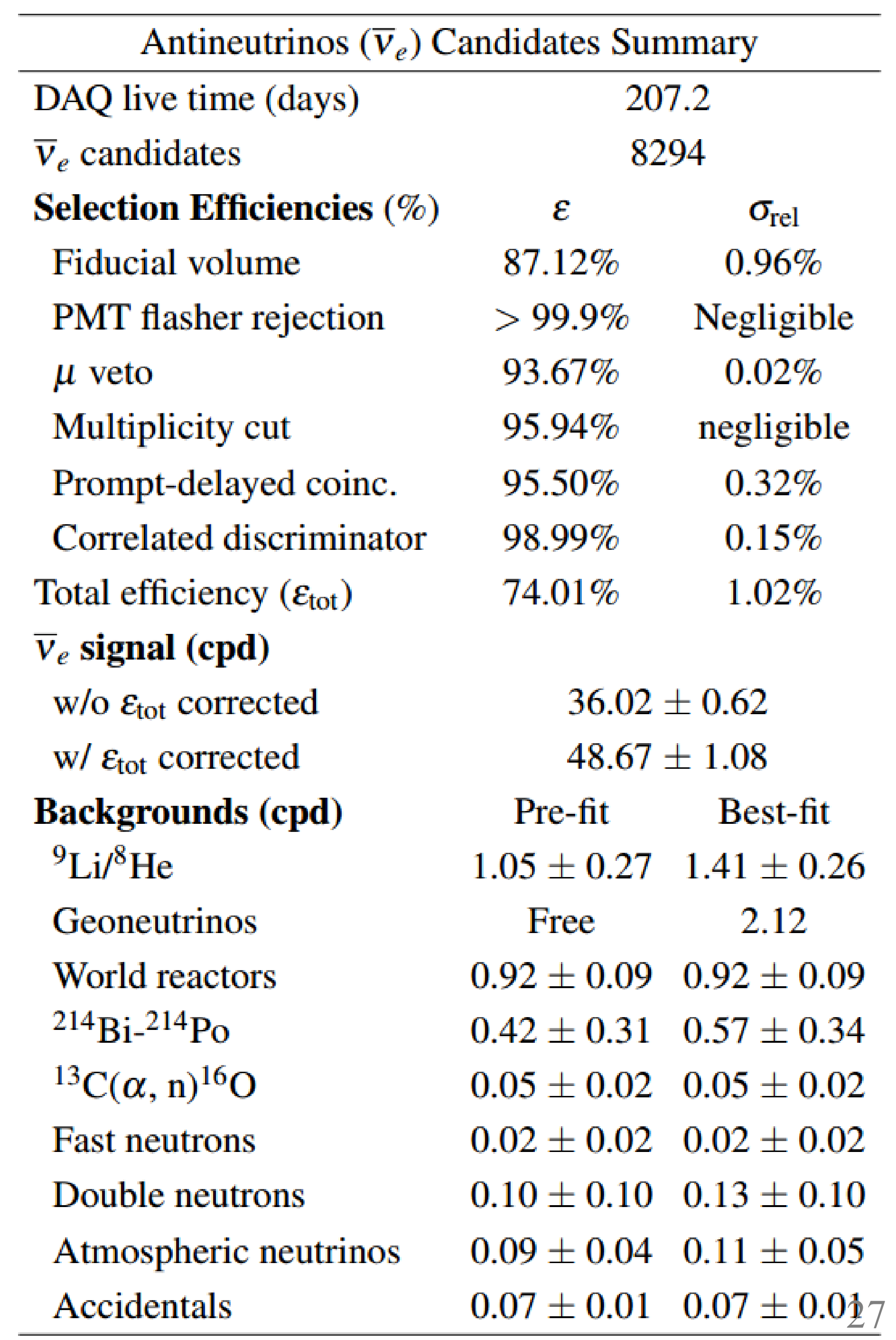

Antineutrinos ($\overline{\nu}_e$) Candidates Summary		
DAQ live time (days)	207.2	
$\overline{\nu}_e$ candidates	8294	
Selection Efficiencies (%)	ε	σ_{rel}
Fiducial volume	87.12%	0.96%
PMT flasher rejection	> 99.9%	Negligible
μ veto	93.67%	0.02%
Multiplicity cut	95.94%	negligible
Prompt-delayed coinc.	95.50%	0.32%
Correlated discriminator	98.99%	0.15%
Total efficiency ($\varepsilon_{\mathrm{tot}}$)	74.01%	1.02%
$\overline{\nu}_e$ signal (cpd)		
w/o $\varepsilon_{\mathrm{tot}}$ corrected	36.02 ± 0.62	
w/ $\varepsilon_{\mathrm{tot}}$ corrected	48.67 ± 1.08	
Backgrounds (cpd)	Pre-fit	Best-fit
^{9}Li/^{8}He	1.05 ± 0.27	1.41 ± 0.26
Geoneutrinos	Free	2.12
World reactors	0.92 ± 0.09	0.92 ± 0.09
^{214}Bi-^{214}Po	0.42 ± 0.31	0.57 ± 0.34
^{13}C(α, n)^{16}O	0.05 ± 0.02	0.05 ± 0.02
Fast neutrons	0.02 ± 0.02	0.02 ± 0.02
Double neutrons	0.10 ± 0.10	0.13 ± 0.10
Atmospheric neutrinos	0.09 ± 0.04	0.11 ± 0.05
Accidentals	0.07 ± 0.01	0.07 ± 0.01

New Results of Solar Oscillation Parameters

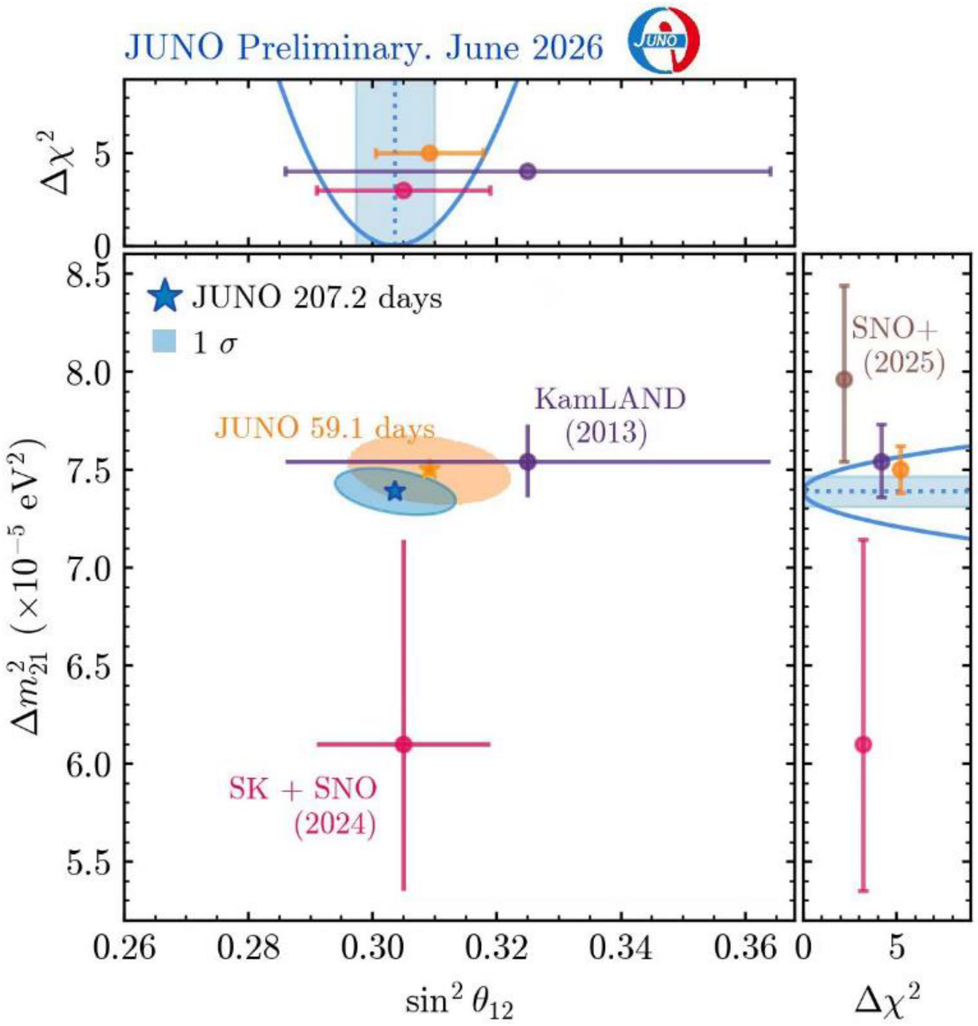

Δm^2_{21}	7.388 ± 0.078 (1.60% → 1.06%)
$\sin^2\theta_{12}$	0.3036 ± 0.0064 (2.8% → 2.1%)

- Even though the statistical uncertainty is dominant, systematic errors become important:
  - ⇨ ^{214}Bi bkg. and detection eff. can be improved

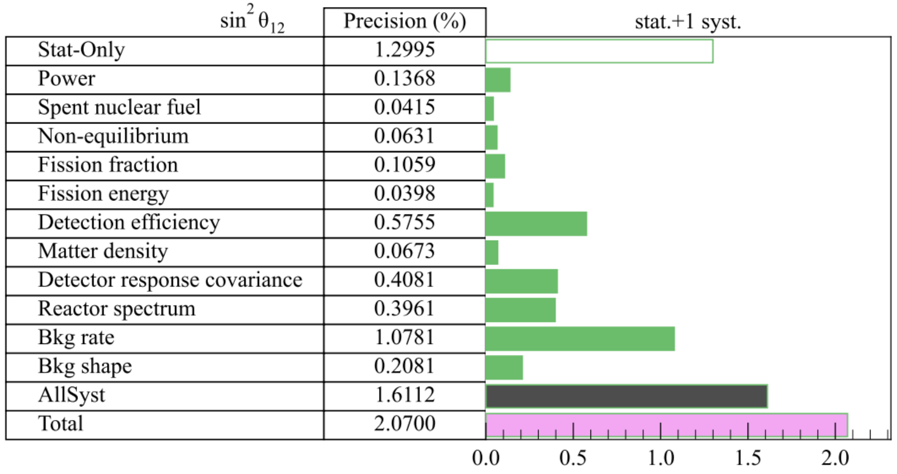

$\sin^2\theta_{12}$	Precision (%)
Stat-Only	1.2995
Power	0.1368
Spent nuclear fuel	0.0415
Non-equilibrium	0.0631
Fission fraction	0.1059
Fission energy	0.0398
Detection efficiency	0.5755
Matter density	0.0673
Detector response covariance	0.4081
Reactor spectrum	0.3961
Bkg rate	1.0781
Bkg shape	0.2081
AllSyst	1.6112
Total	2.0700

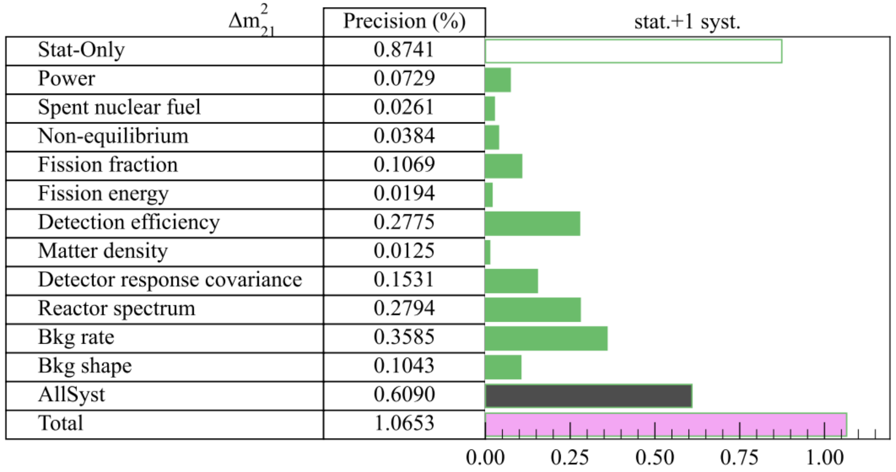

Δm^2_{21}	Precision (%)
Stat-Only	0.8741
Power	0.0729
Spent nuclear fuel	0.0261
Non-equilibrium	0.0384
Fission fraction	0.1069
Fission energy	0.0194
Detection efficiency	0.2775
Matter density	0.0125
Detector response covariance	0.1531
Reactor spectrum	0.2794
Bkg rate	0.3585
Bkg shape	0.1043
AllSyst	0.6090
Total	1.0653

First Result of Δm^2_{31}

Posters: 252, 205

- Due to statistical fluctuations, JUNO only profiles of Δm^2_{31} have multiple minima

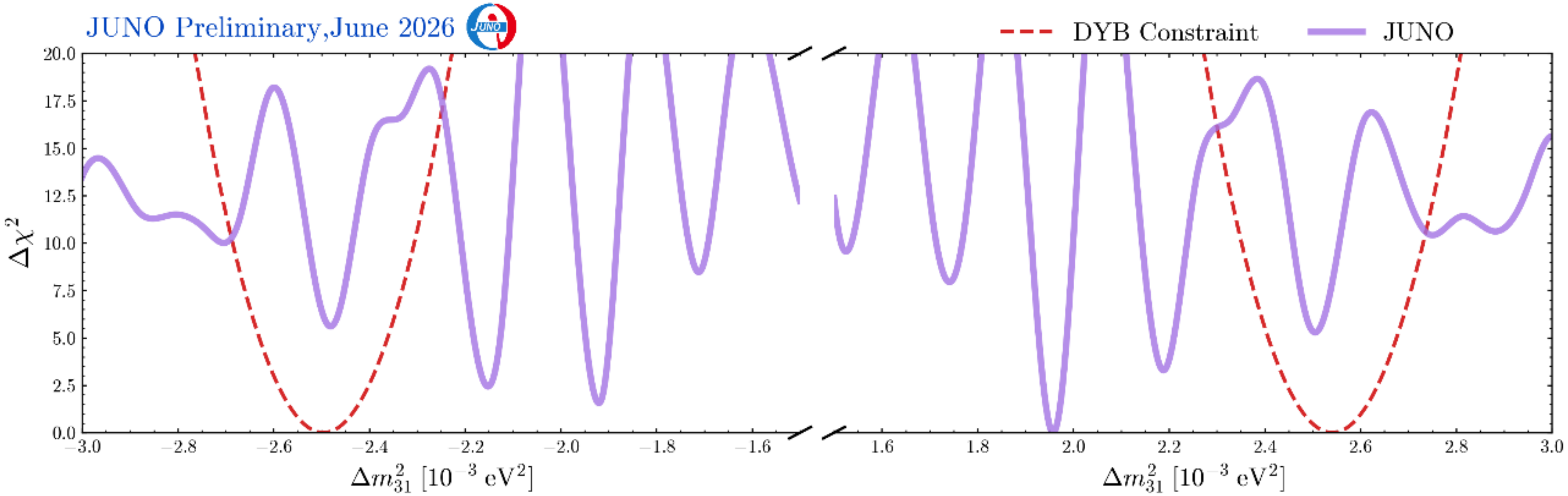

The final minimum for each mass ordering is obtained by using the Δm^2_{31} constraint from the Daya Bay result (PRL 130 16, 161802)

Feldman-Cousins (FC) method is used to determine the 1σ range of Δm^2_{31}: ~1% precision achieved

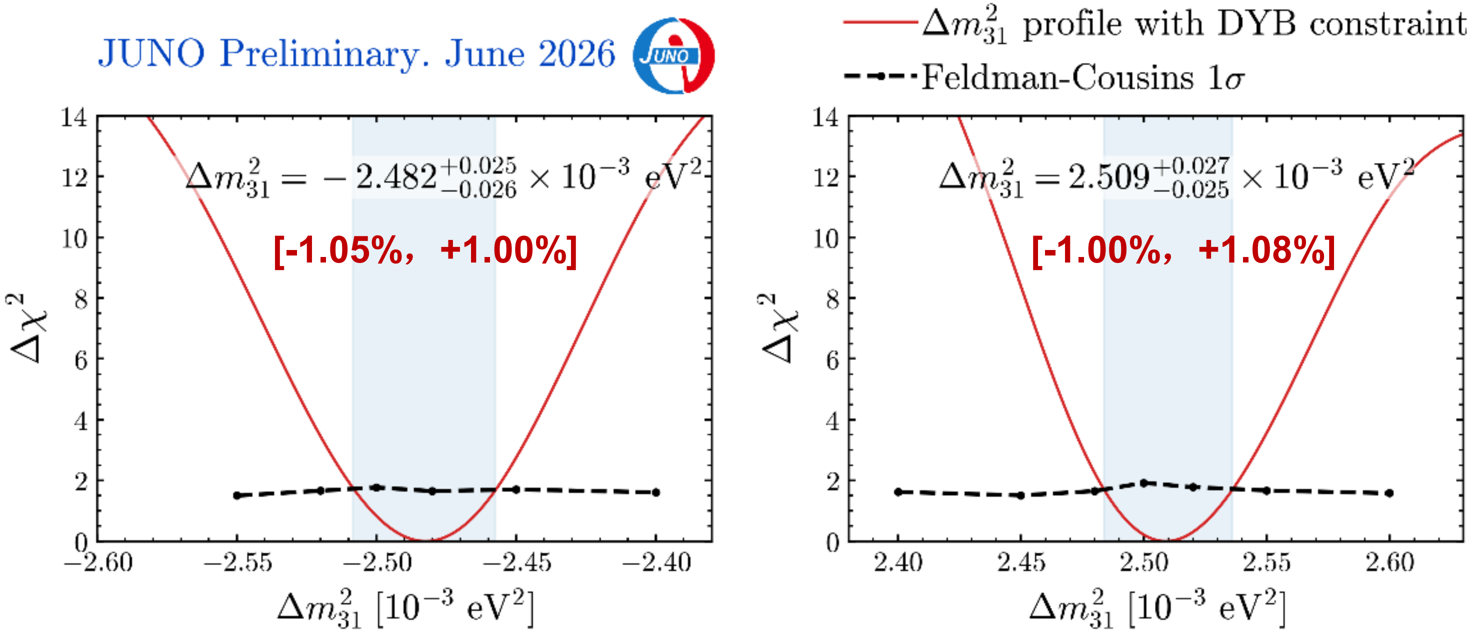

Adding Constraint from NuFit-LBL

Posters: 252, 205

- Δm^2_{31} from reactor and accelerator neutrinos should align at the right mass ordering[1]
- Adopt the NuFit-LBL results from [2]: normal mass ordering is favored at $\Delta\chi^2 = 4.86$

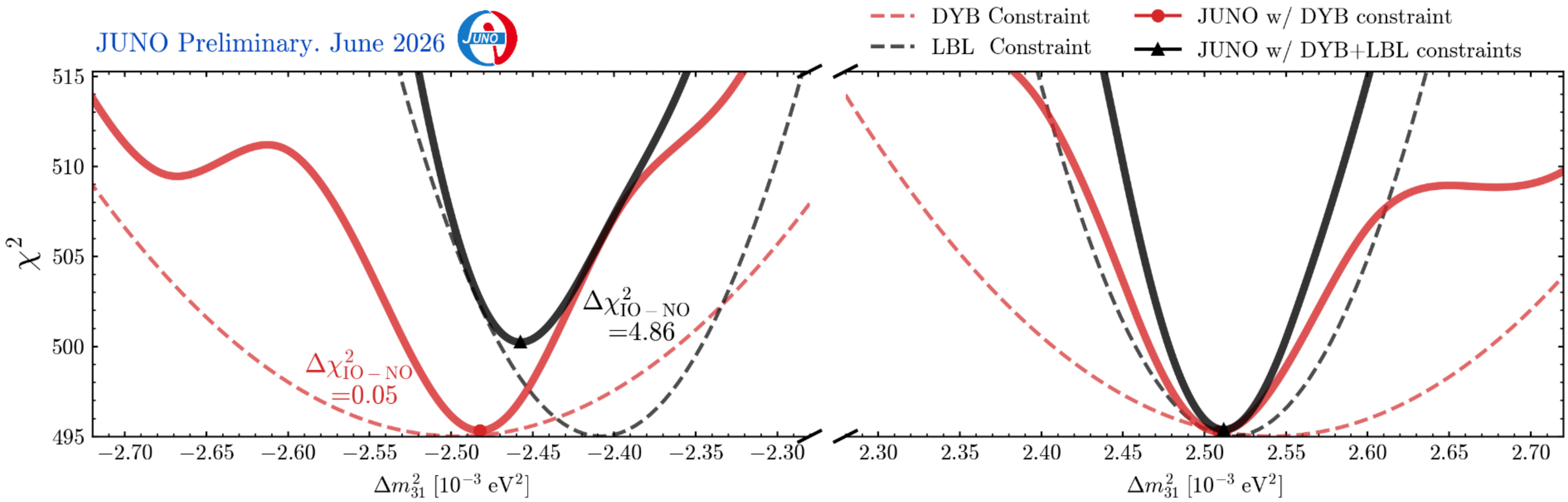

[1] H. Nunokawa, S. Parke and R.Z. Funchal, Phys. Rev. D 72 (2005) 013009; Y. F. Li et al., Phys. Rev. D 88, 013008 (2013)

[2] NuFIT 6.0 (JHEP 12 (2024) 216 [arXiv:2410.05380]), www.nu-fit.org and M. Maltoni private communication

Neutrino Mass Ordering Significance

Posters: 252, 205

- Frequentist approach using pseudo exp. to convert $\Delta\chi^2$ to significance
- Influence of δ_{CP} considered (scanned)
- Normal Ordering is favored at **2.3σ**

- Bayesian approach using Markov Chain Monte Carlo(MCMC) method
- Normal Ordering is favored with a Bayes factor of **10.18** ➔ 2ln κ= 4.64
  - ⇨ Consistent with the frequentist $\Delta\chi^2$

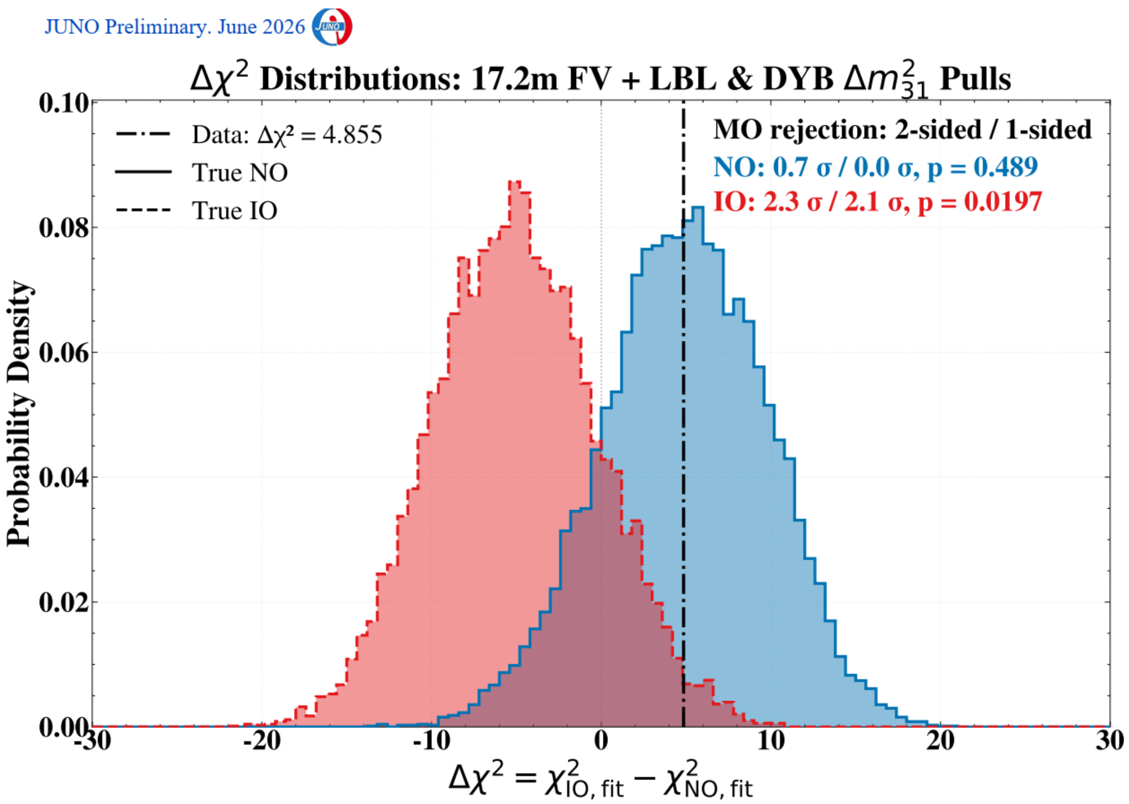

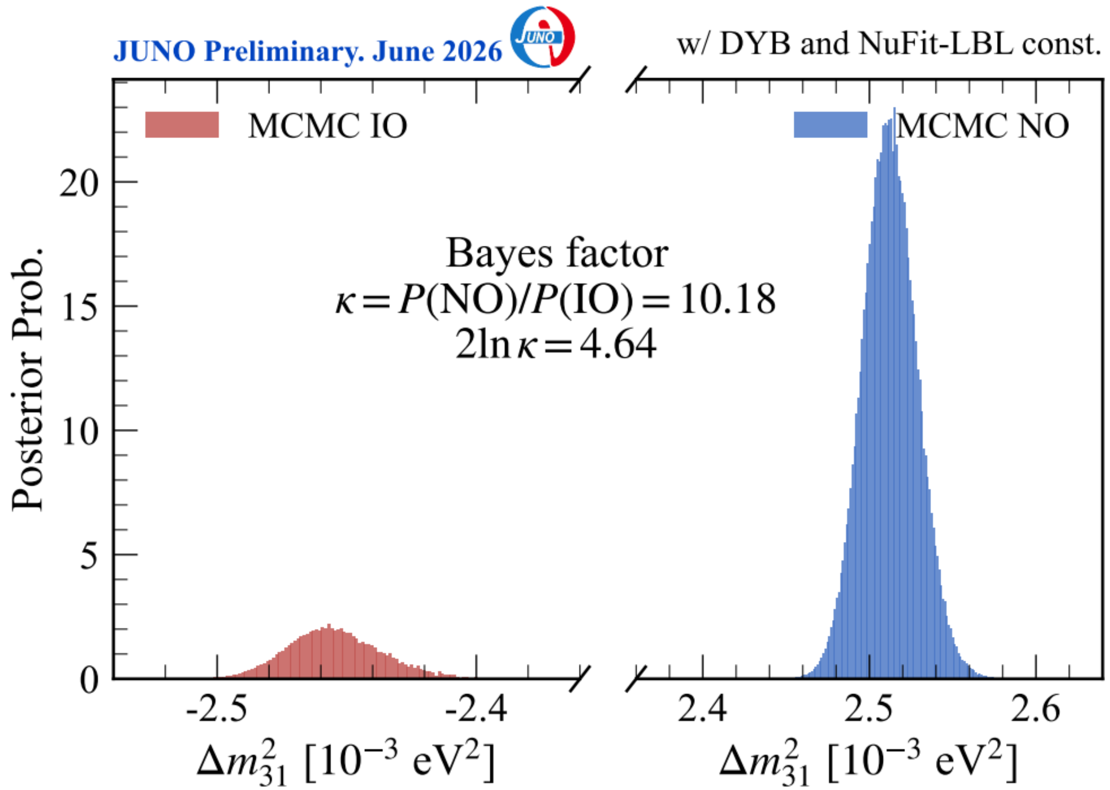

Consistent Results from Independent Analyses

- **Our 3 independent analyses got consistent results (0.2σ)**
  - ⇨ different event reconstruction code, fiducial volume, selection cuts, efficiency, background estimation, energy response models and oscillation fitters

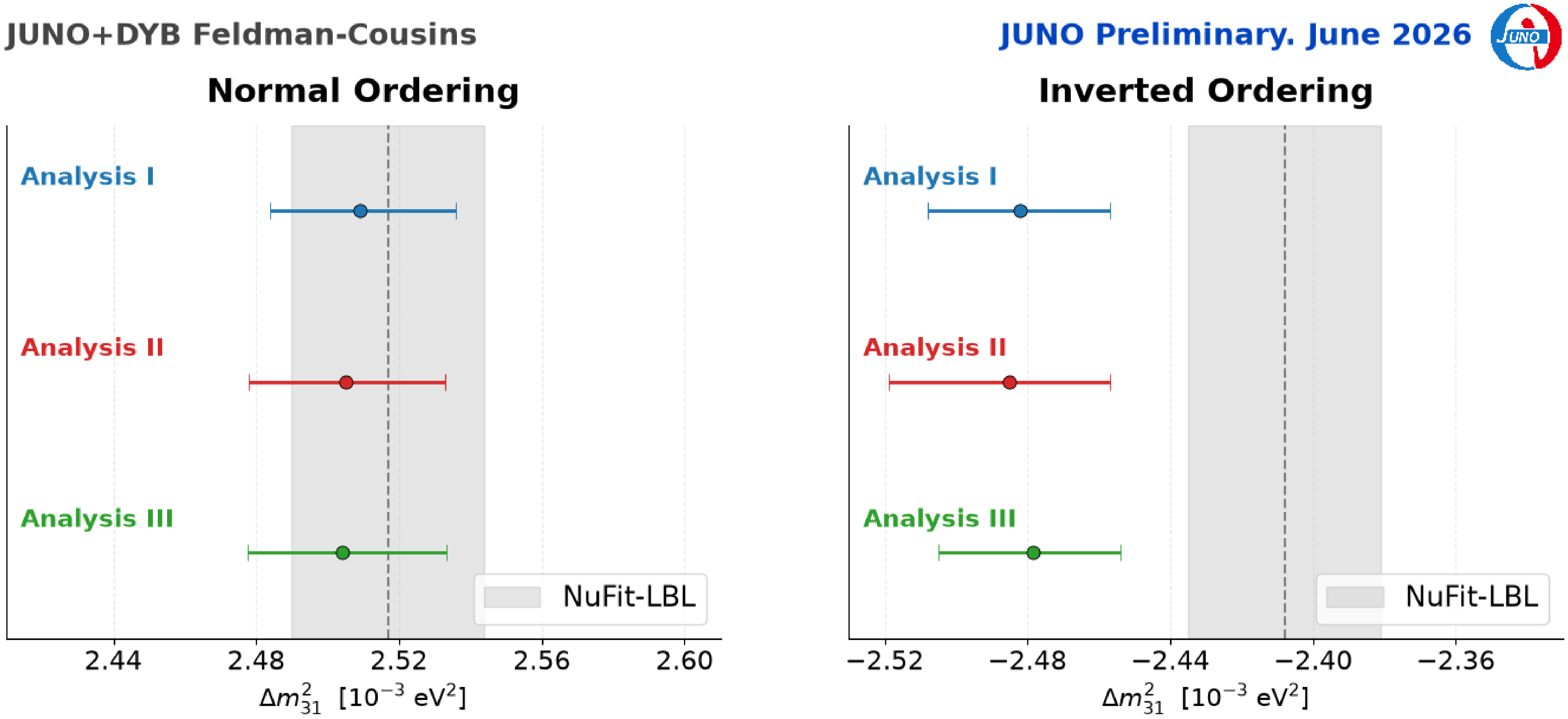

Comparison of Results on Oscillation Parameters

$\sin^2 2\theta_{12}$

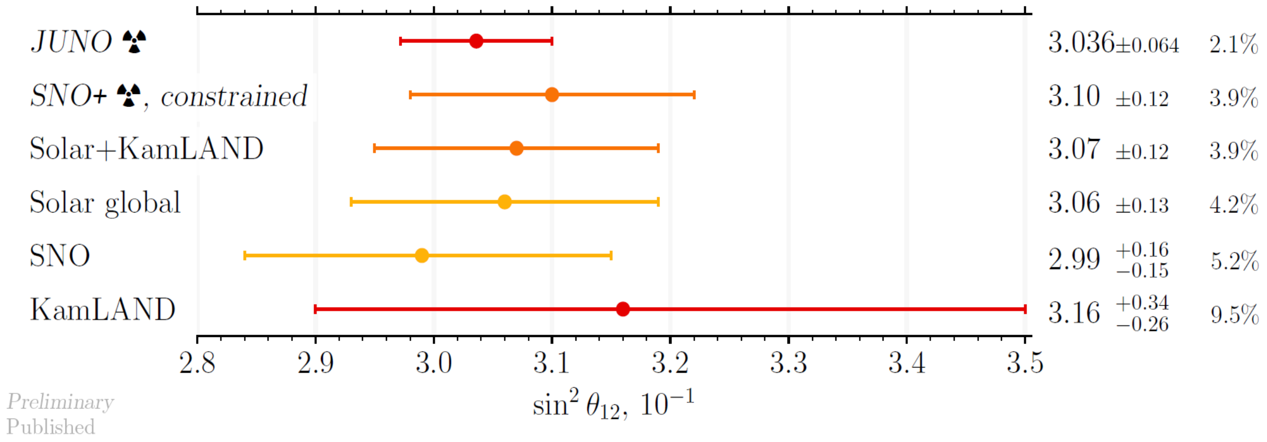

Δm^2_{21}

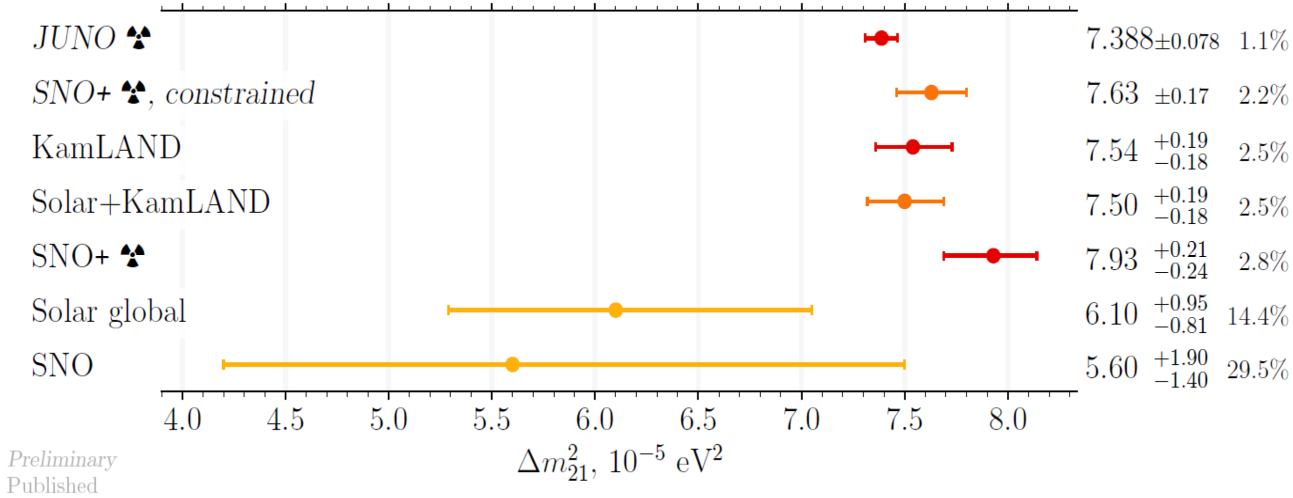

Results from JUNO have smallest uncertainties

Δm^2_{31}

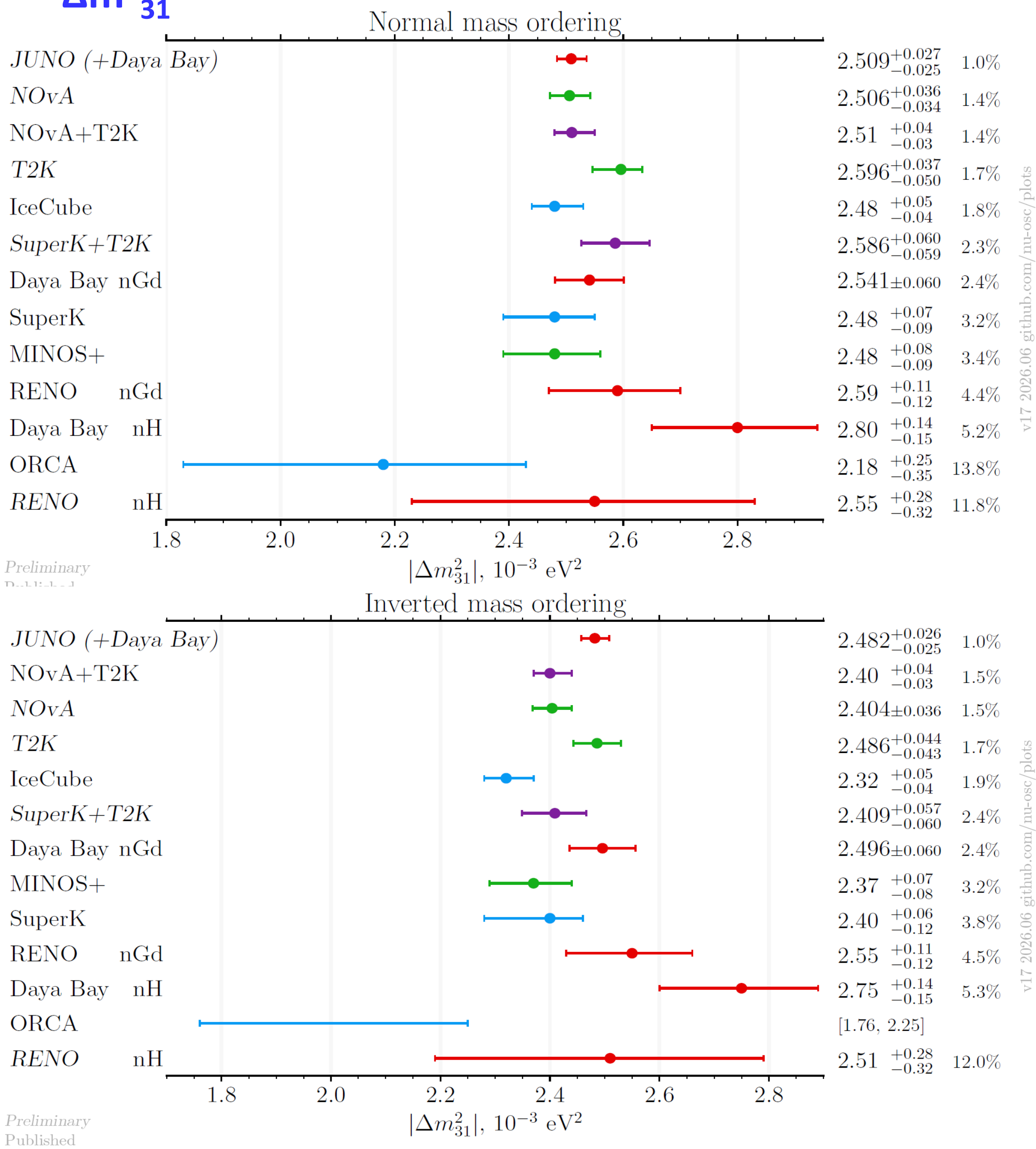

New Results on Geo-neutrinos

Poster: 341

- Fits are performed without constraint on geo-neutrino flux, but with 3.4±10% U/Th ratio
  - ⇨ Constraining the geo-nu flux doesn't change oscillation results
- Clear geo-nu signals at 1-3 MeV, giving a flux of 73 ± 11 TNU
  - ⇨ Largest geo-neutrino samples so far, and most precise measurement
- JUNO result is higher than expectation from existing models, but not statistically significant
- Need more JUNO data and more refined geological model predictions

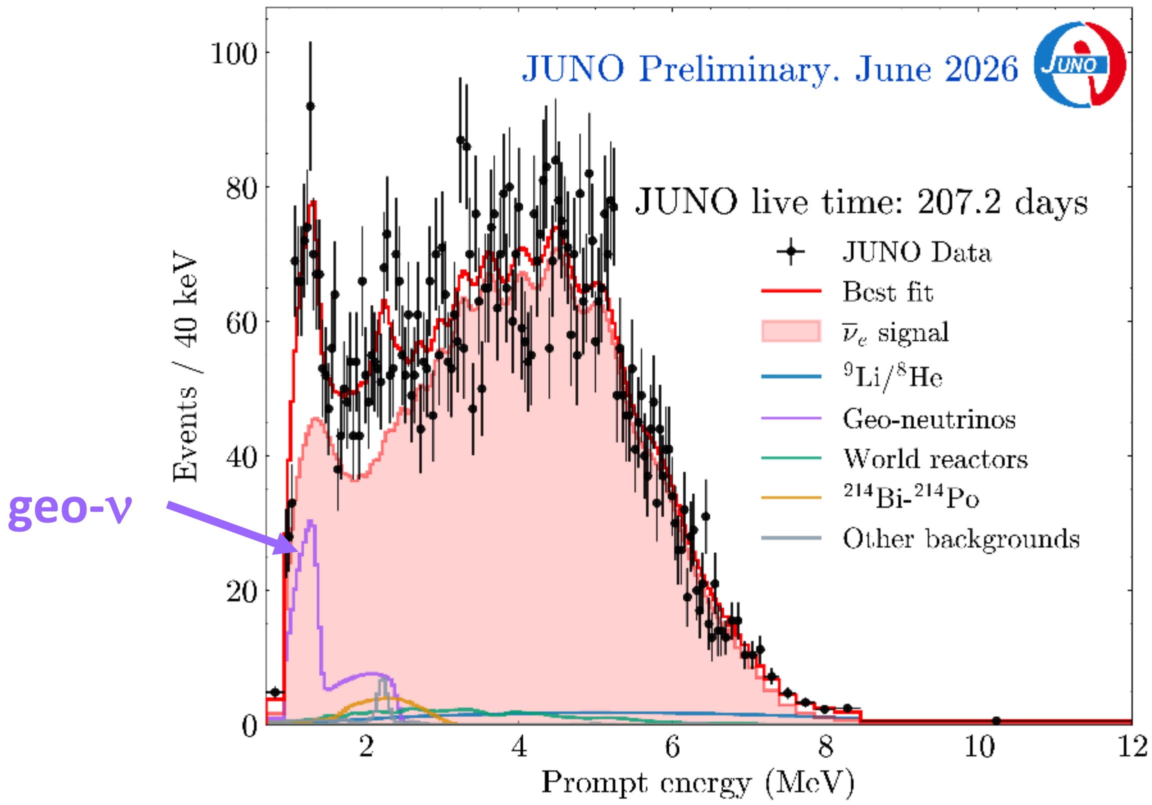

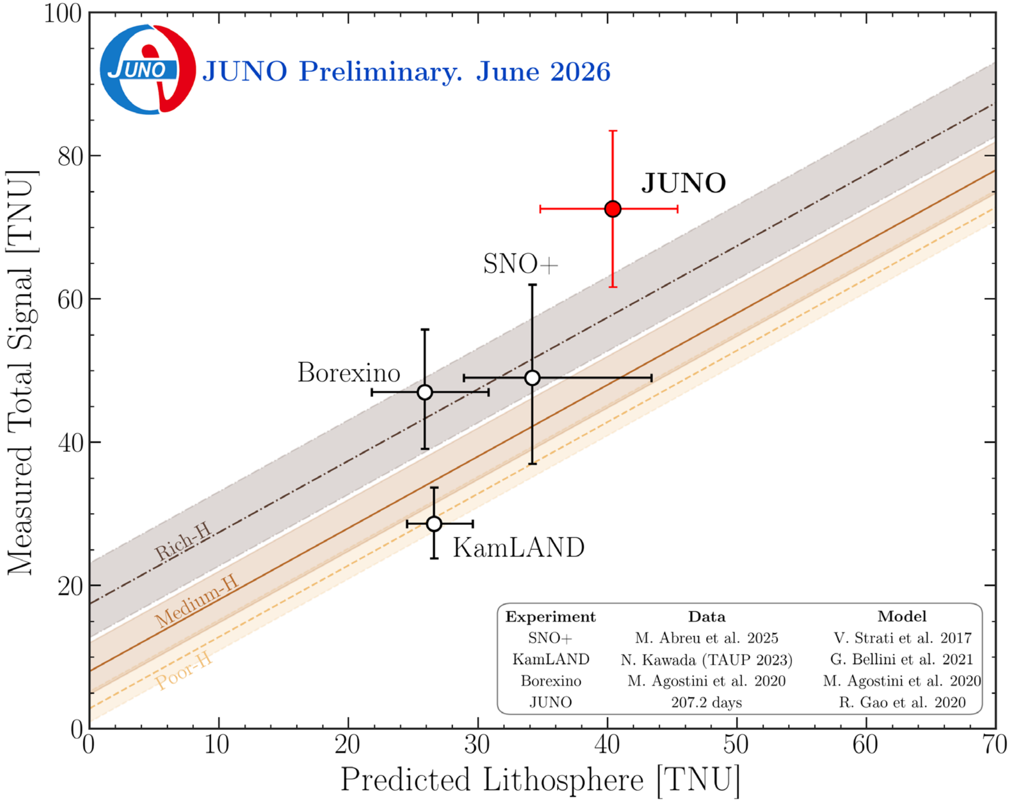

Experiment	Data	Model
SNO+	M. Abreu et al. 2025	V. Strati et al. 2017
KamLAND	N. Kawada (TAUP 2023)	G. Bellini et al. 2021
Borexino	M. Agostini et al. 2020	M. Agostini et al. 2020
JUNO	207.2 days	R. Gao et al. 2020

Posters

#	Topics	Poster Title	Poster ID
1	Reactor	Inverse beta-decay selection, efficiency estimation and accidental background calculation in JUNO's oscillation measurement	346
2	Reactor	Fiducial volume and target proton systematic uncertainties in JUNO's Reactor Antineutrino Oscillation Measurement	328
3	Reactor	Muon Veto Optimization for the Reactor Neutrino Oscillation Measurements in JUNO	357
4	Reactor	Cosmogenic background estimation for JUNO's oscillation parameter measurement	273
5	Reactor	First Geoneutrino Measurement at JUNO	341
7	Reactor	Fitting Framework for JUNO's Reactor Antineutrino Oscillation Analysis	252
8	Reactor	Constraining the reactor antineutrino spectrum in JUNO's oscillation measurement	205
9	Reactor	214Bi-214Po Background of Reactor Antineutrino Oscillation Measurement and Rn Control in JUNO Detector	404
11	Solar - bkg	Radioactive backgrounds determination in the JUNO liquid scintillator	344
12	Solar	Study of cosmogenic isotopes in view of B8 neutrinos at JUNO	284
13	Solar	B-8 Solar Neutrino in JUNO water phase	17
14	CCSN/MM	The Multi-messenger Trigger System for JUNO Experiment	266
15	CCSN/MM	Realization of Core-Collapse Supernova Monitoring System at JUNO	199
16	Atmo	First atmospheric neutrino signal observed in JUNO	264
17	GANYMEDE	Comprehensive prediction of atmospheric neutrino neutral-current background at JUNO	201
18	Atmo	JUNO Sensitivity to DSNB Signal	430

Posters

19	TAO	Precision measurement of reactor neutrino spectrum of TAO	371
20	TAO	Performance of the JUNO TAO Central Detector	483
21	TAO	Muon related background at JUNO-TAO	250
22	TAO	Channel-level SiPM calibration at JUNO-TAO	223
23	TAO	Performance of the Veto System for JUNO-TAO	246
24	Reco	COTI and Deconvolution Waveform Reconstruction in JUNO	419
25	Reco	Neural Network-Based Waveform Reconstruction in JUNO	345
26	Reco	Event vertex reconstruction in JUNO	#
27	Reco	Energy reconstruction in JUNO	272
28	Reco	Measurement of the Carbon-14 Rate in JUNO Liquid Scintillator and Implications for Pile-Up Identification	323
29	Reco	Identification and Suppression of Radioactive Emissions from PMT Glass for Enhanced JUNO Energy Resolution	162
30	Reco	Cosmic Muon Track Reconstruction in JUNO	128
31	Reco	Machine-Learning–Based Reconstruction of Atmospheric Neutrino Events in the JUNO Liquid Scintillator Detector	432
32	Calib	JUNO 20" LPMTs charge, timing and DCR calibration	347
33	sPMT	Calibration of the LPMT Non-Linearity and SPMT Low-Level Performance in JUNO	340
34	Calib	Energy Response Model of the JUNO Central Detector	334
35	Calib	JUNO Detector Energy Resolution in Physics Data-Taking Phase	406
36	Calib	JUNO Liquid Scintillator Attenuation Measurement	337
37	Calib	Cosmogenic Neutron Studies in JUNO	335

Posters

38	Production/Software	JUNO data production	354
39	Simulation	Simulation of the JUNO experiment: challenges, description and comparison with data	270
41	OEC	Online Event Classification in JUNO	254
42	DQ	Data Quality Monitoring System of JUNO Experiment	343
43	sPMT	Energy resolution and calibration with the small PMT system of JUNO	370
44	Veto	The muon tracker of the JUNO experiment	283
45	Veto	JUNO Water Cherenkov Detector and performance	325
46	LS	The production of JUNO LS	324
47	LS	Towards Future Upgrades of JUNO: Quantitative Cherenkov–Scintillation Separation Studies Enhancing Background Suppression for Rare Events Search	373
48	LS/OSIRIS	Design and hardware of the OSIRIS radiopurity monitor for JUNO	171
49	LS/OSIRIS	OSIRIS' results on radioactive background levels in the JUNO scintillator	363
50	LPMT	Instrumentation and Operational Status of the JUNO 20-inch PMT System	220
51	LPMT	Standalone Measurement of Afterpulses in 20-inch PMTs for the JUNO Experiment	218
53	Offline	Offline Software and DCI System of JUNO Experiment	359
54	Calibration	Calibration system of the JUNO experiment	248
55	Calibration	Calibration source 3-D positioning in JUNO	249
56	DAQ	JUNO DAQ System	338
57	DCS	Detector Control and High-Voltage System for the JUNO Neutrino Experiment	48

Summary

- The JUNO detector and TAO are successfully built and operating smoothly
- Initial performance shows that the detector works well as designed
- Precision of solar oscillation parameters further improved by a factor of 1.3-1.5
- First measurement on Δm^2_{31} achieved a precision of ~1%
- With external constraint, **Normal Mass Ordering** is favored at ~2.3σ
- First geo-neutrino results yield a flux of 73 ± 11 TNU
- Other promising new results not covered in this talk:
  - ⇨ First atmospheric neutrino events in JUNO, poster-264, 201
  - ⇨ First limit on the DSNB neutrino flux in JUNO, poster-430
  - ⇨ Smooth running of supernova neutrino alert system, poster-266, 199
  - ⇨ Solar neutrino background modelling, poster-344, 284, 17

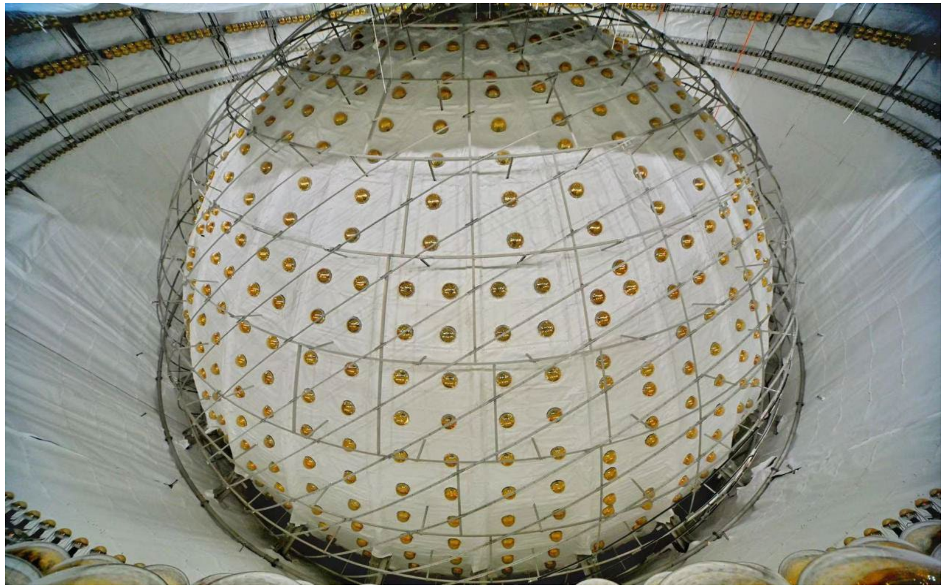

Backup

Atmospheric Neutrinos and DSNB

Poster ID: 264, 430, 432

- Selected 8.8 ± 0.4 day^{-1} fully-contained atmospheric neutrinos in LS (first time)
  - ⇨ Rate and energy spectrum consistent with expectation
- Work in progress, more to come: flux and oscillation physics, NC interaction…

Preliminary

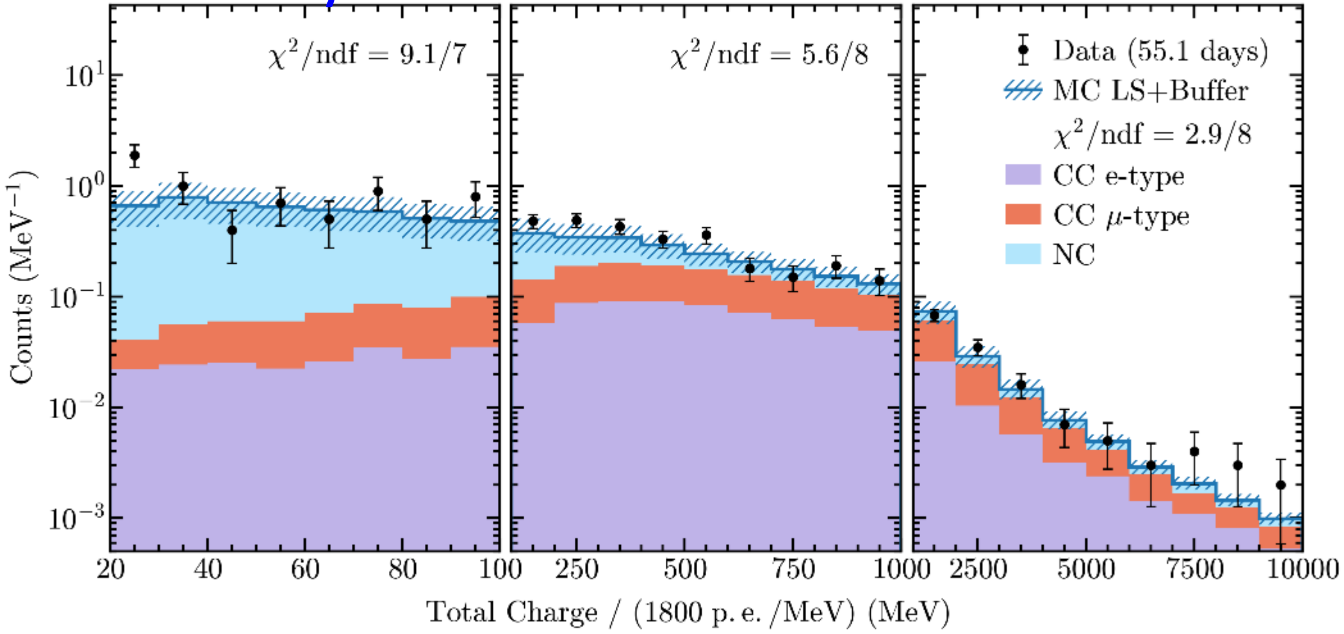

- 19 events observed in (12-30 MeV) as Diffused Supernova Neutrino Bkg.(DSNB) candidates
  - ⇨ Agree with bkg. prediction: 21.3 ±10.5
  - ⇨ Competitive flux upper limit is given
- PSD study suggests that they are mostly atmo. ν

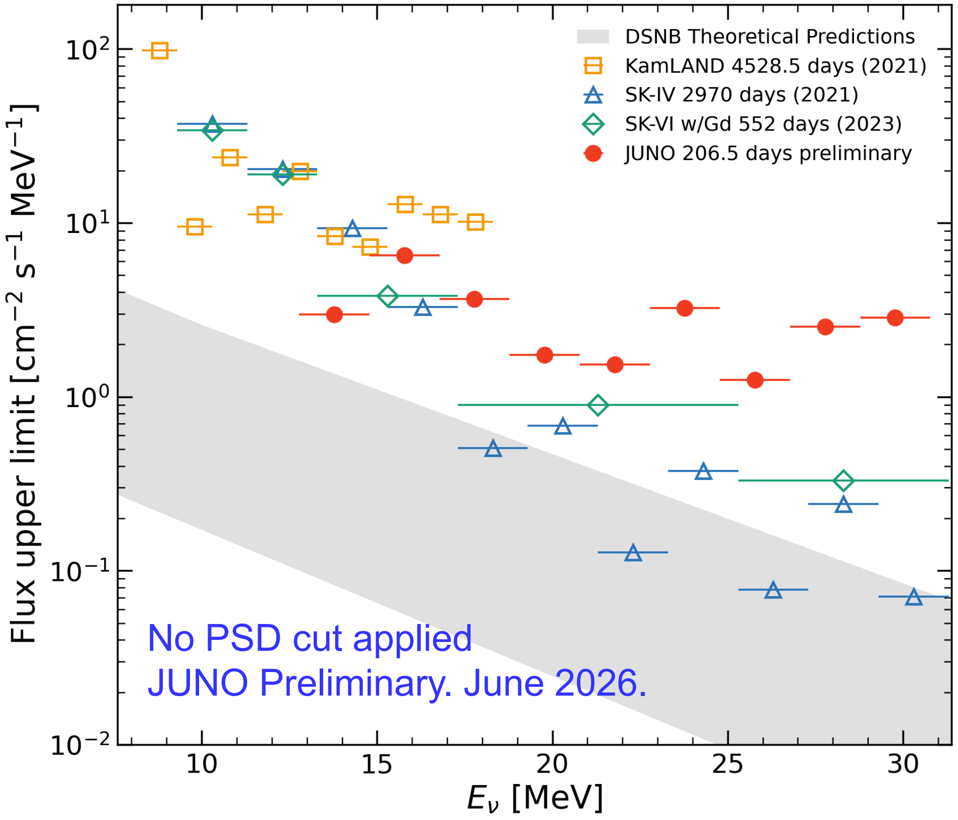

No PSD cut applied
JUNO Preliminary. June 2026.